U.PORTO
FEUP FACULDADE DE ENGENHARIA
UNIVERSIDADE DO PORTO

AN INDUSTRIALLY-VALIDATED AUTOMATED MODAL ANALYSIS METHOD APPLIED TO THE MONITORING OF THE INFANTE ARCH-BRIDGE

MARCO ALVES BARREIRA

Dissertation submitted for partial fulfilment of the requirements for the degree of
MASTER IN CIVIL ENGINEERING — SPECIALIZATION IN STRUCTURES AND GEOTECHNICS

Supervisor: Professor Doctor Carlos Manuel Ramos Moutinho

Co-Supervisor: Professor Doctor Filipe Manuel Rodrigues Leite Magalhães

Responsible at Siemens: Engineer André Guilherme Massano Tavares

JUNE 2024

MASTER IN CIVIL ENGINEERING 2023/2024

CIVIL ENGINEERING DEPARTMENT

Tel. +351-22-508 1901

m.ec@fe.up.pt

Edited by

FACULDADE DE ENGENHARIA DA UNIVERSIDADE DO PORTO

Rua Dr. Roberto Frias

4200-465 PORTO

Portugal

Tel. +351-22-508 1400

feup@fe.up.pt

http://www.fe.up.pt

To my family,

Se podes olhar, vê. Se podes ver, repara.

José Saramago.

ACKNOWLEDGEMENTS

My accomplishments during my academic journey and this dissertation are all due to the collective support of many people who have come into my life at different times. Each of them has made a significant difference from the moment they entered, and I owe my gratitude to all of them for being by my side.

First, I want to express my gratitude to FEUP, particularly to my supervisor, Professor Carlos Moutinho, and my co-supervisor, Professor Filipe Magalhães, for all their support throughout the entire process and for making my participation in this project thesis possible.

I am also grateful to Siemens Industry Software NV, Leuven, Belgium, for providing me this opportunity and for hosting me. Special thanks go to Engineer André Tavares, who closely accompanied this thesis, for all his support, time, and excellent feedback, which were crucial for the successful conclusion of this project.

To those who journeyed alongside me during this international experience, transforming from mere colleagues into great companions: this adventure in Leuven would have lacked meaning without your presence. You not only made Leuven home but also filled it with precious moments.

To my friends, the ones that I met before and during my tenure at FEUP, I just want to thank you for all the memories and moments that we experienced together.

To the ones who were part of my IACES journey, for all the moments and all the learnings.

To my beloved friends Vítor, Luís, Paulo, and Catarina, for all the moments that we lived together and for all the support, I owe my gratitude.

To my dear friend Susana, with whom I shared this experience at Siemens, thank you for your companionship and support.

To my good friends Romeu, Francisco, and Tiago, I want to extend a special thanks for the difference you made during this process, even without knowing it.

To AHBVCM and all its members, thank you for the memorable moments and insightful knowledge.

Lastly, but most importantly, I want to express my deepest gratitude to my family, who have been with me throughout my entire journey and have provided unwavering support. In particular, I am grateful to my mother, Isabel, and father, Joaquim, for their endless encouragement and support. To my older brother, Pedro, and my sister-in-law, Jéssica, who have always been there for me, I am truly thankful.

I want to give heartfelt acknowledgment to my brother, Leandro, whose companionship has been a guiding light since the very beginning of this journey. And to my cousin, Dévora, for her constant presence and support throughout my life.

ABSTRACT

Modal analysis is an excellent technique for determining the natural vibration characteristics of a structure. By understanding modal parameters such as natural frequencies, damping ratios, and mode shapes, engineers can fully characterize a structure's dynamic behaviour, predicting performance and identifying potential issues. This technique is applicable in various fields, including civil engineering, aerospace, and automotive industries, where it aids in improving design, performance, and ensuring structural integrity. Nonetheless, the process can be time-consuming and heavily reliant on user subjectivity in selecting modal parameters. As structural complexity escalates, interpreting stabilization diagrams becomes increasingly challenging, necessitating expert-level knowledge for accurate analysis. Additionally, performing modal analysis on large infrastructures for long-term monitoring is often impractical due to these challenges.

Considering the challenges of traditional modal analysis, this work develops an Automated Modal Analysis (AMA) methodology using a density-based machine learning clustering technique, coupled with modal verification steps inspired by expert judgment. This approach aims to minimize user interaction, reduce human error, and decrease the time required for the process. Consequently, it enables long-term monitoring of structures without significant effort.

In this thesis, AMA methodology was initially validated within an Experimental Modal Analysis (EMA) context. The methodology was applied to eight distinct industrial datasets, ranging from simple structures like a metallic plate to more complex ones such as an F16 jet. This validation aimed to assess the methodology's applicability across diverse structural scenarios. Additionally, a benchmark validation study, incorporating results from manually selected modes by engineers of varied expertise levels, was conducted to bolster the obtained findings.

In the context of Operational Modal Analysis (OMA), the AMA methodology developed in this work was applied to the Infante Dom Henrique bridge in Porto for long-term monitoring purposes. This application aimed to demonstrate the methodology's effectiveness in real-world scenarios.

In this thesis, expert-level results were achieved in the jury test conducted for benchmark validation, affirming the efficacy of the proposed AMA methodology. Additionally, successful long-term monitoring of the bridge was achieved, demonstrating the methodology's viability in both EMA and OMA contexts. Overall, the study highlights the successful implementation of the AMA methodology across diverse modal analysis scenarios.

KEYWORDS: Automated Modal Analysis, Industrial Validation, Jury Test, Long-term Monitoring, Arch-Bridge.

RESUMO

A análise modal é uma excelente técnica para determinar as características naturais de vibração de uma estrutura. Ao compreender os parâmetros modais, como frequências naturais, amortecimento e formas modais, os engenheiros podem caracterizar completamente o comportamento dinâmico de uma estrutura, prevendo o desempenho e identificando potenciais problemas. Esta técnica é aplicável em várias áreas, incluindo engenharia civil, aeroespacial e indústrias automóveis, onde ajuda a melhorar o design, o desempenho e a garantir a integridade estrutural. No entanto, o processo pode ser demorado e depender fortemente da subjetividade do utilizador na seleção dos parâmetros modais. Conforme a complexidade estrutural aumenta, a interpretação dos diagramas de estabilização torna-se cada vez mais desafiadora, exigindo conhecimento especializado para uma análise precisa. Além disso, realizar análise modal em grandes infraestruturas para monitorização a longo prazo é frequentemente impraticável devido a estes desafios.

Considerando os desafios da análise modal tradicional, neste trabalho desenvolve-se uma metodologia de Análise Modal Automática (AMA) utilizando uma *density-based machine learning clustering technique*, aliada a etapas de verificação modal baseadas em estudos anteriores. Esta abordagem visa minimizar a interação do utilizador, reduzir erros humanos e diminuir o tempo necessário para o processo. Consequentemente, possibilita a monitorização a longo prazo de estruturas sem um esforço significativo.

Nesta tese, a metodologia de AMA foi inicialmente validada no contexto da Análise Modal Experimental (EMA). A metodologia foi aplicada a oito conjuntos de dados industriais distintos, que variaram desde estruturas simples como uma placa metálica até estruturas mais complexas, como um avião F16. Esta validação teve como objetivo avaliar a aplicabilidade da metodologia em diversos cenários estruturais. Além disso, um estudo de validação de benchmark, incorporando resultados de modos selecionados manualmente por engenheiros de diferentes níveis de experiência, foi conduzido para reforçar os resultados obtidos.

No contexto da Análise Modal Operacional (OMA), a metodologia AMA desenvolvida neste trabalho foi aplicada à ponte Infante Dom Henrique, no Porto, para fins de monitorização a longo prazo. Esta aplicação teve como objetivo demonstrar a eficácia da metodologia em cenários do mundo real.

Nesta tese, foram alcançados resultados de nível de especialista no *Jury Test* realizado para validação de benchmark, confirmando a eficácia da metodologia proposta de AMA. Além disso, foi alcançada uma monitorização bem-sucedida a longo prazo da ponte, demonstrando a viabilidade da metodologia em contextos de EMA e OMA. No geral, o estudo destaca a implementação bem-sucedida da metodologia AMA em diversos cenários de análise modal.

PALAVRAS-CHAVE: Análise Modal Automática, Validação Industrial, Jury Test, Monitorização a Longo Prazo, Ponte.

CONTENTS

List of Figures

LIST OF TABLES

Symbols, Acronyms and Abbreviations

Acronyms

EMA – Experimental Modal Analysis

OMA – Operational Modal Analysis

NVH – Noise Vibration Harshness

AMA – Automated Modal Analysis

MPE – Modal Parameter Estimation

AMPS – Automated Modal Parameter Selection

AMT – Automated Modal Tracking

FDD – Frequency Domain Decomposition

SSI – State-Space Identification

p-LSCF – Polyreference Least Squares Complex Frequency

FCM – Fuzzy C-Means

DBSCAN – Density-Based Spatial Clustering of Applications with Noise

OPTICS – Ordering Points to Identify the Clustering Structure

HDBSCAN – Hierarchical Density-Based Spatial Clustering of Applications with Noise

FRFs – Frequency Response Functions

UR – Upper Residues

LR – Lower Residues

CPS – Cross-Power Spectra

ACF – Autocorrelation function

CCS – Cross-correlation function

APSD – Auto-power spectral densities

MAC – Modal Assurance Criterion

Symbols

f – natural frequency [Hz]

ξ – damping ratio [%]

ϕ – mode shapes

H – System transfer function

N – Number of modes

Q_r – Modal scaling factor

$\{\Psi\}$ – Modal vector

λ – System pole

N_m – Number of modes

B – Numerator matrix polynomial

A – Denominator matrix polynomial

Ω_r – Polynomial basis functions

Δt – Sampling time

$\alpha_r,\ \beta_r$ – Coefficients

$[I]$ – Identity matrix

p – Pole

N_p – Number of poles

d – distance

N_c – Number of clusters

L – Modal participation factors

N_o – Number of outputs

N_i – Number of inputs,

m – Mode

H_{error} – FRF synthesis error

H^s – FRF synthesis for a chosen modeset M

H^m – measured FRF

Abbreviations

PolyMax - Polyreference Least Squares Complex Frequency

MinPts – Minimum number of points

rp – Representative poles

minRef_contribution – Minimum reference contribution

limDubPolCheck – Limit contribution to start doubting about a cluster

difPolesRef – fraction of poles that a cluster must have to be classified as a physical cluster

1
INTRODUCTION

1.1. MOTIVATION

Modal analysis became a critical important topic in what concerns to the analysis of structural dynamics and their characterization, commonly used to studying the behaviour of mechanical and civil structures (Chen, W. [et al.], 2011). Experimental modal testing has been a commonly used technique to identify the modal parameters of large engineering structures. However, this method requires knowledge of both input and output data, which can be challenging and costly for the analysis of big structures such as bridges, wind turbines, dams, and airplanes. The expense and logistical complexity of performing these tests on large structures often limit their feasibility (Zhang, G. [et al.], 2014).

To address the limitations mentioned above, certain algorithms have been developed that estimate modal parameters using only the structural response to ambient excitation, such as wind or traffic. When both input and output data are available, experimental modal analysis (EMA) can be performed. However, when only the output data is known, the process falls under operational modal analysis (OMA). One of the main advantages of OMA compared to EMA is that it avoids causing damage to the structure. This is because OMA measurements are performed under operational conditions, without interrupting the structure's functionality.

The modal analysis process encompasses several stages, beginning with data acquisition, followed by signal pre-processing and data assessment, and culminating in system identification through the calculation of a valid set of modal parameters. This methodology finds widespread application across various fields, including automotive design and vehicle Noise Vibration Harshness (NVH) testing, prognostics for industrial machinery, monitoring of various civil structures such as bridges, wind turbines, and stadiums, as well as numerous other domains (Tavares, A. [et al.], 2024).

Over the years, many civil structures undergo degradation and are exposed to various dynamic loads, including traffic, wind, or pedestrian activity. As a result, there is a growing need for monitoring systems in such structures, along with a well-planned monitoring programs (de Magalhães, F.M.R.L., 2010).

With the implementation of monitoring systems and the collection of their data, it becomes possible to evaluate the evolution of modal parameters over time using automated modal analysis (AMA) methodologies, as further discussed in the next section. This analysis provides valuable insights into the behaviour of structures, enabling better decision-making regarding their operation, optimizing maintenance scheduling, and predicting end-of-life dates (Steenackers, G. and Guillaume, P., 2005). Ultimately, this enhances the safety of the structure and reduces operational costs (Dederichs, A.C. [et al.], 2022).

Due to the reasons mentioned above, an Automated Modal Analysis (AMA) methodology was developed in this dissertation to monitor the structural response of the Infante Dom Henrique bridge in Porto. To validate the applicability of this AMA methodology across different types of structures, it was applied to various industrial datasets and evaluated through an extensive benchmark comparison with multiple modal analysis engineers.

1.2. STATE-OF-THE-ART

As mentioned earlier in section 1.1, modal analysis is a crucial technique in structural dynamics and vibration engineering. However, as this technique advances and is applied to increasingly complex structures, the process becomes more time-consuming and prone to human error. Automating modal analysis is essential to address these challenges. It enables engineers of all expertise levels to create precise modal models for a wide variety of structures. Furthermore, automation allows for the efficient processing of large datasets with consistent results and minimal user intervention. (Tavares, A. [et al.], 2024).

Automated modal analysis (AMA) consists of three steps: a) Modal Parameter Estimation (MPE), b) Automated Modal Parameter Selection (AMPS), c) Automated Modal Tracking (AMT).

In the past years, numerous variants for modal parameter estimation of structures have been studied. Parameter estimation can be performed using time domain functions, which process data based on the input-output time histories, or frequency domain functions, which estimate the modal parameters based on the frequency domain representation of the input-output relationships. (Heylen, W. and Sas, P., 2006). The time domain functions are not the focus of this study, which relies only on frequency domain functions.

In the frequency domain functions, there are some methods implemented, like the frequency domain decomposition (FDD) (Brincker, R. [et al.], 2000), the State-Space Identification (SSI) methods (Peeters, B. and De Roeck, G., 1999) (Boonyapinyo, V. and Janesupasaeree, T., 2010) (Zhang, G. [et al.], 2012) and the polyreference least-squares complex frequency-domain (p-LSCF) (Peeters, B. [et al.], 2007).

Most AMPS techniques use clustering approaches after processing the frequency domain functions. These clustering methods create clusters to identify the modal parameters of the structure. The hierarchical clustering is one of the most commons to proceed with the AMPS methodology (Verboven, P. [et al.], 2004). Other types of centroid-based clustering algorithms, as K-means and fuzzy c-means (FCM) clustering also had relevance in the development of the AMPS (Favarelli, E. and Giorgetti, A., 2020) (Reynders, E. [et al.], 2012) (Verboven, P. [et al.], 2002). Different approaches as the density-based clustering techniques are being applied too, like the Density-Based Spatial Clustering of Application with noise (DBSCAN) (Tavares, A. [et al.], 2024) and Ordering Points to Identify the Clustering Structure (OPTICS) (Teng, J. [et al.], 2019). Another type of clustering technique was also developed based in the hierarchical and density-based clustering approaches, the Hierarchical DBSCAN (HDBSCAN) (Campello, R.J. [et al.], 2013).

After the AMPS process, Automated Modal Tracking (AMT) allows for understanding the evolution of the structural modal parameters over time. This is valuable not only for recognizing the structural mode parameters but also for identifying significant variations (Dederichs, A.C. and Øiseth, O., 2024). The AMT methodology can be performed based on the calculation of distances, where the most common parameters to proceed to the tracking are the natural frequency and the Modal Assurance Criterion (MAC). This procedure can be performed based on the calculation of the distances between the two parameters mentioned above, as was done in a concrete arch dam by (Pereira, S. [et al.], 2020). Alternatively, it can be based solely on the frequency as demonstrated in a bridge study by (Teng, J. [et al.], 2019). Other parameters can also be used, as shown in the work by (He, M. [et al.], 2022).

AMA methodologies are becoming highly relevant due to their accuracy and speed in processing modal parameters without user interaction. These procedures can be implemented in modal analysis softwares as an add-on, allowing users to utilize this method to streamline the process (Rainieri, C. [et al.], 2008, Tavares, A. [et al.], 2023).

1.3. Objectives

The main objectives of this dissertation are:

- Improvement of an in-house Automated Modal Analysis (AMA) methodology based on a density-based clustering technique (Tavares, A. [et al.], 2023).
- Validation of the AMPS method proposed conducted on 8 industrial datasets within an experimental modal analysis (EMA) context through a Benchmark Validation study.
- Extra validation in a case of operational modal analysis (OMA), on the Infante Dom Henrique bridge.
- Application of the AMA approach in the Infante Dom Henrique Bridge, for the monitoring of modal parameters across time.

1.4. Thesis Outline

The present dissertation is divided in six chapters.

Chapter 1 outlines the main motivations behind this work and provides context for the subsequent chapters. It also includes a list of objectives to guide the research.

Chapter 2 is constituted by the theoretical background that sustains the topics discussed in the next chapters. The modal analysis theory, such as the modal model, the Polyreference Least Squares Complex Frequency Domain, the difference between the Experimental and Operational modal analysis and the modal assurance criterion. Moreover, the theory behind DBSCAN algorithm is also explained.

Chapter 3 holds the process behind the automated modal analysis methodology to be further validated in the two upcoming chapters. The method is divided into two main parts, the automated modal parameter selection, and the automated modal tracking.

Chapter 4 starts with a brief explanation of the industrial datasets used to corroborate the automated modal parameter selection method presented in section 3.1, as well as the results. The chapter also presents the results of the benchmark study conducted using the industrial datasets.

Chapter 5 begins with a description of the geometry and the monitoring system implemented in the Infante Dom Henrique bridge. Following this, the methodology presented in chapter 3 is implemented to further validate the methodology and proceed to the identification of the modal parameters of the structure.

Chapter 6 provides the final conclusions and some ideas for future work.

2

THEORETICAL BACKGROUND

2.1. MODAL ANALYSIS

Modal Analysis is the study of the dynamic behaviour of a structure, providing a set of modal parameters such as natural frequencies (f), damping ratios (ξ) and mode shapes (ϕ) (Avitabile, P., 2017). This technique can be applied to several industrial scenarios.

In the field of modal analysis, it is possible to determine the modal parameters with two techniques: experimental modal analysis (EMA) and operational modal analysis (OMA). EMA involves providing a known excitation to the structure and measuring the response. In contrast, OMA performs modal analysis using only the output data, with the assumption of white noise excitation. A detailed explanation of these two techniques is provided in later sections.

2.1.1. MODAL MODEL

In the procedure of measuring the modal parameters, the Frequency Response Functions (FRFs) obtained are curved-fitted by a modal model (Heylen, W. and Sas, P., 2006) present in equation (2.1).

$$[H(j\omega)] = \sum_{r=1}^{N} \frac{Q_r \{\Psi\}_r \{\Psi\}_r^t}{(j\omega - \lambda_r)} + \frac{Q_r^* \{\Psi\}_r^* \{\Psi\}_r^{*t}}{(j\omega - \lambda_r^*)} \tag{2.1}$$

Where, N is the number of modes; Q_r the modal scaling factor; $\{\Psi\}_r$ the modal vector r; λ_r the system pole, that can be defined by the natural frequency f_r and the damping ratio ξ_r, as defined in equation (2.2) (Heylen, W. and Sas, P., 2006).

$$\lambda_r, \lambda_r^* = -\xi_r f_r \pm j\sqrt{1 - \xi_r^2} f_r \tag{2.2}$$

In the field of experimental modal analysis, the study is typically conducted over a limited frequency band that encompasses only a subset of the structure's modes. This limitation arises from the constraints of the Frequency Response Functions (FRF) matrix, which includes a finite subset of inputs and outputs (de Magalhães, F.M.R.L., 2010). As a result of this limitation, the modal model for a specific frequency band is defined in equation (2.3).

$$[H(j\omega)] = \sum_{k=1}^{N_m} \frac{\{\phi_k\}\langle\, l_K^T\rangle}{(j\omega - \lambda_r)} + \frac{\{\phi_k^*\}\langle\, l_K^H\rangle}{(j\omega - \lambda_r^*)} + UR - \frac{LR}{\omega^2} \tag{2.3}$$

where N_m is the number of modes in the frequency band under analysis; $\{\phi_k\}$ are the mode shapes; $\cdot^*, \cdot^T, \cdot^H$ are the conjugate, transpose, and the complex conjugate transpose of a matrix, respectively; $\langle\, l_K^T\rangle$ are the modal participation factors. UR (Upper Residues) and LR (Lower Residues) represents the influence of the modes below (LR) and above (UR) the frequency band. These residues can be defined in various ways, depending on the measured output quantity, such as displacement, velocity, or acceleration (NV, S.I.S., 2015).

2.1.2. Polyreference Least Squares Complex Frequency Domain (p-LSCFD)

The polyreference least-squares complex frequency-domain method, commonly referred to as "PolyMax" is a frequency-domain parameter estimation method that can be implemented in two steps. Firstly, the construction of the stabilization diagram involves gathering frequency, damping, and participation information. Then, based on the selection of stable poles from this diagram, the mode shapes are determined. (Peeters, B. [et al.], 2004).

With the first input being frequency response functions (FRFs), this method identifies a matrix-fraction model shown in equation (2.4).

$$[H(\omega)] = [B(\omega)][A(\omega)]^{-1} \tag{2.4}$$

Where, $H(\omega)$ is a matrix that contains the FRFs between all the inputs and outputs, $B(\omega)$ is de numerator matrix polynomial and $A(\omega)$ is the denominator matrix polynomial. Each row in right matrix-fraction model can be represented as represented in equation (2.5).

$$\forall 0 = 1,2,\dots,l\colon \langle H(\omega)\rangle = \langle B_0(\omega)\rangle[A(\omega)]^{-1} \tag{2.5}$$

Where the numerator row-vector polynomial of output (O) and the denominator matrix polynomial are defined as presented in equation (2.6) and (2.7), respectively.

$$\langle B_0(\omega)\rangle = \sum_{r=0}^{p} \Omega_r(\omega)\langle\beta_{or}\rangle \tag{2.6}$$

$$[A(\omega)] = \sum_{r=0}^{p} \Omega_r(\omega)[\alpha_r] \tag{2.7}$$

Where p is the polynomial order, and $\Omega_r(\omega)$ are the polynomial basis functions. When a z-domain model is used, $\Omega_r(\omega)$ should be considered as shown in equation (2.8) (Δt is the sampling time).

$$\Omega_r(\omega) = e^{j\omega\Delta tr} \tag{2.8}$$

In the process of solving the set of equations presented, the coefficient β_r is eliminated, with the focus solely on determining α_r. This last coefficient provides an estimate of the system poles and the modal participation factor (Heylen, W. and Sas, P., 2006).

To control the parameter redundancy in the right matrix-fraction formulation (equation (2.4)) is defined one constrain, $[\alpha_r] = [I]$.

In Figure 2.1 it is possible to visualize a PolyMax stabilization diagram provided by Simcenter™ Testlab™ software. PolyMax provides very clear stabilization diagrams that make very simple selection of the physical modes. Another advantage of the method is the estimation of the non-physical modes with a negative damping, what permits the previous elimination of this modes before the construction of the stabilization diagram (Peeters, B. [et al.], 2004).

The basic idea behind a stabilization diagram involves conducting multiple iterations of the complete pole identification process, employing models of increasing order. Through extensive experience across diverse problem sets, it was observed that the pole values corresponding to "physical" eigenmodes consistently appear around a nearly identical frequency. Conversely, mathematical poles tend to disperse across the frequency spectrum. By consolidating the pole values obtained from analyses at various orders into a single diagram, with the pole frequency on the horizontal axis and the solution order on the vertical axis, a comprehensive visualization is achieved. Physical poles are distinctly visible in this diagram. The poles can be categorized using different letters, as illustrated in Figure 2.1, based on how many stability criteria they meet. Typically, these stability criteria include 1% for frequency, 5% for damping, and 2% for eigenvector stability. The letter 'f' denotes a pole stable in frequency, 'd' indicates stability in damping, 'o' signifies a newly-discovered pole, 'v' represents stability in both frequency and modal participation vector, and 's' indicates stability across all criteria. (Lau, J. [et al.], 2007).

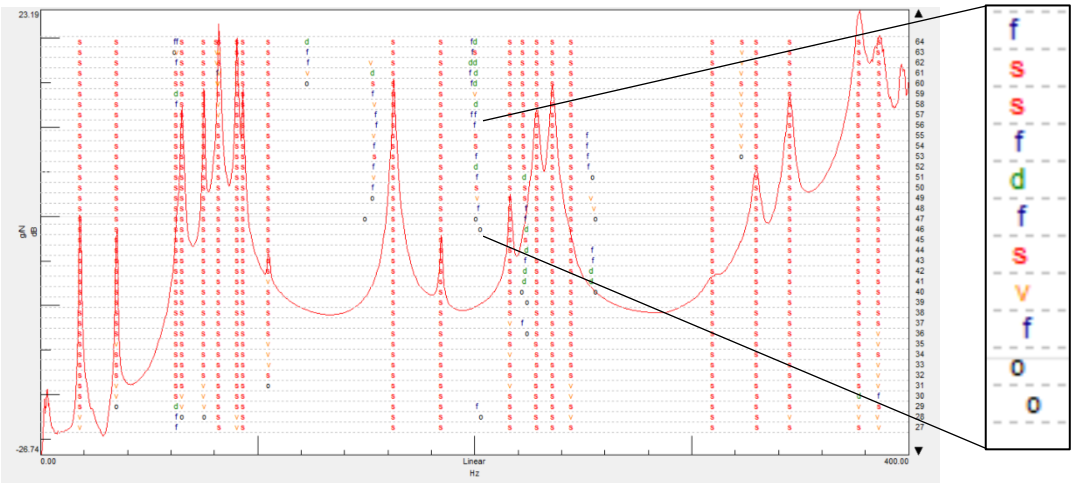

Figure 2.1 - Example of a stabilization diagram in Siemens Simcenter™ Testlab™ software.

In the present work the utilized software to implement PolyMax was MATLAB. In Figure 2.2 it is possible to see a stabilization diagram provided by MATLAB, where the blue dots represent the stable poles, and the red curve, the sum of the measured FRFs with the main resonance peaks (Tavares, A. [et al.], 2024).

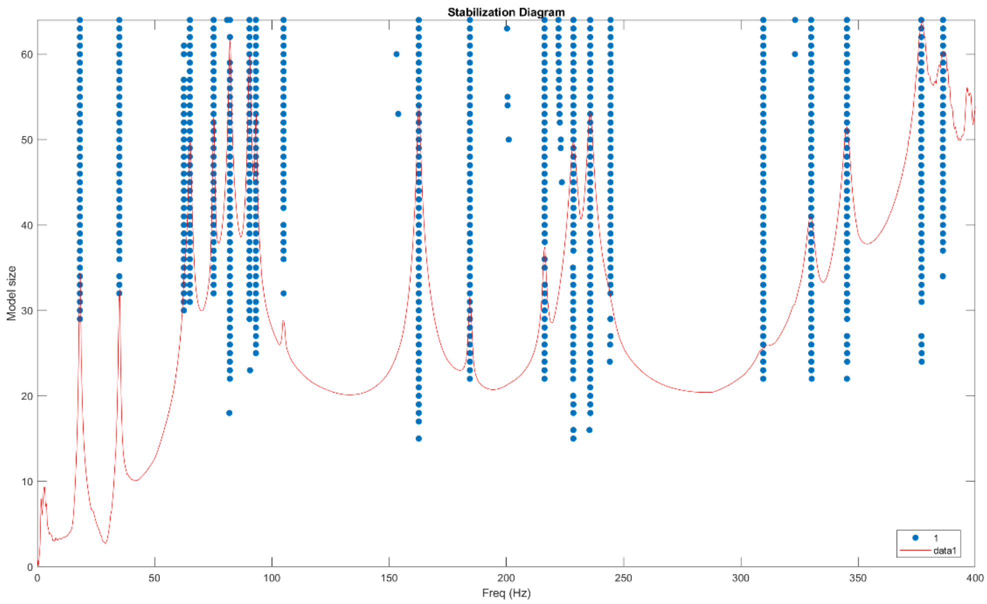

Figure 2.2 – Example of a stabilization diagram in MATLAB.

2.1.3. Experimental Modal Analysis Vs. Operational Modal Analysis

Experimental modal analysis and Operational modal analysis, also known as EMA and OMA, respectively, are methods that use measured data to build a mathematical model of the structure's dynamic characteristics. This model is built based in a family of frequency-domain functions.

For EMA, PolyMax or other frequency-domain modal parameter estimators calculate the stabilization diagrams with respect to the Frequency Response Functions (FRF), a frequency domain representation of the relation between input and output response of a structure. In contrast, for OMA, Cross-Power Spectra (CPS) functions are used, which are calculated with respect to the cross and auto-correlation functions between the output-only data. The main difference between the two processes is the characterization of the system transfer function, H. In Figure 2.3, it is possible to see the summary of both methods.

In EMA, as already was referred above, through the interpretation of FRFs and stabilization diagrams it is possible to estimate the modal parameters of a physical structure. These FRFs are obtained calculating the frequency ratio between the inputs and outputs of the measurements, and for this reason it is necessary to know both input and output forces. This last one, can be presented as acceleration, velocity, or displacement.

Overall, these functions represent the structure response in each measurement location per unit force at the input location. As complex frequency domain functions, FRFs have magnitude and phase information.

One of the particular advantages of EMA is the possibility to represent each mode shape rightly mass-normalized or arbitrarily scaled, and to calculate the modal participation factors, due to the fact that the input force is known (Center, S.S., 2020b).

Considering the challenges associated with accessing the input of large infrastructures, such as Civil Engineering structures, where conducting Experimental Modal Analysis (EMA) may necessitate costly and cumbersome equipment (Magalhães, F. and Cunha, Á., 2011), Operational Modal Analysis (OMA) emerges as a practical alternative. OMA is an output-only method, relying on white noise input. By assuming this input condition, OMA characterizes the response solely through "ambient" excitation sources like wind or traffic (Brincker, R. and Ventura, C., 2015). This approach enables the analysis of structures under operational conditions, as they are naturally stimulated in real-world environments without the need for additional excitation devices. Moreover, OMA allows the continuous monitoring (Di Lorenzo, E., 2017).

Due to the white noise assumption is also possible to define the mathematical model that permits the calculation of the modal parameters. In this case, as the input force is unknown, it is impossible to define the FRFs in the same way as EMA, so with the response is possible to create time domain functions, known as correlations functions. The method works knowing only the response, such as accelerations signals.

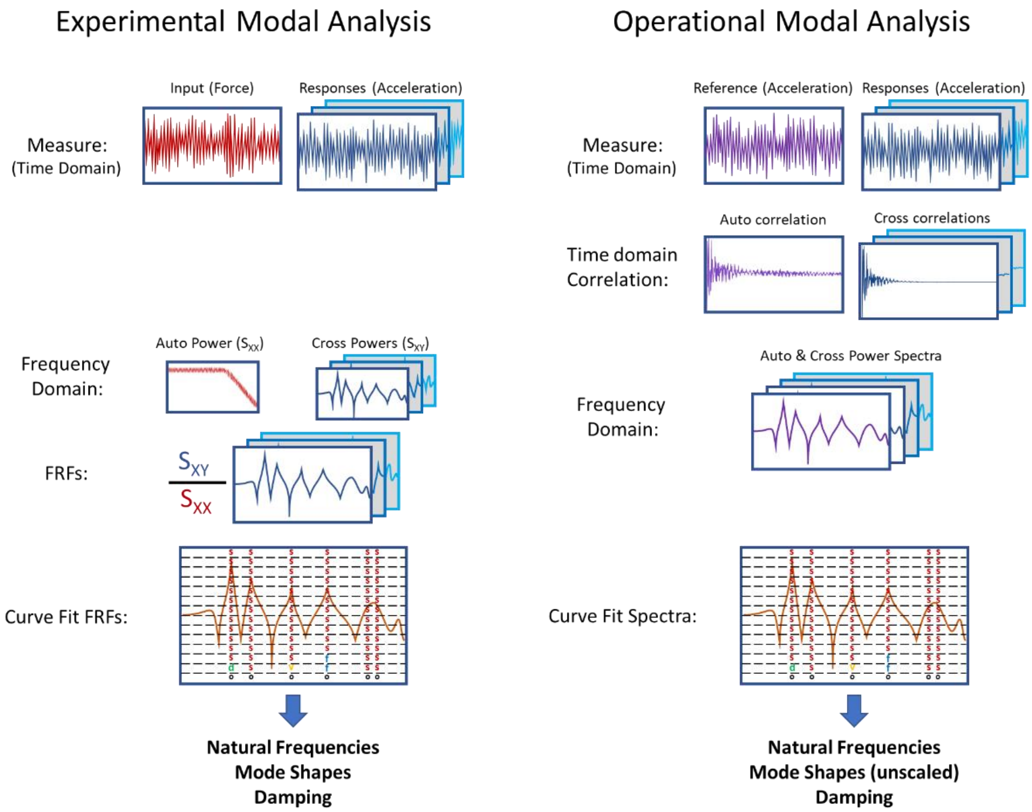

Figure 2.3 - Summary of EMA vs. OMA processes (Center, S.S., 2020b).

In a simple explanation, OMA is based on the structure response [Y] and in the assumption of the white noise, to be able to characterize the structure, as is possible to see in Figure 2.4, based in this two known parameters it is possible to reconstruct the signal in the frequency domain, using an autocorrelation function (ACF) or a cross-correlation function (CCS).

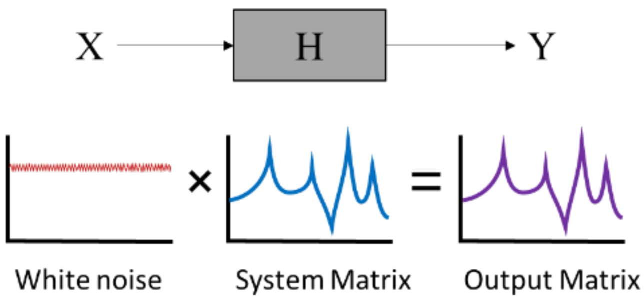

Figure 2.4 - For white noise input, output matrix [Y] is equal to system matrix [H] (Center, S.S., 2020b).

An ACF is a statistical function that quantifies the correlation between two a signal and a delayed copy of itself as a function of delay, providing a value between -1 and 1. If the original signal includes periodic components, like natural frequencies, the delay version of the signal will exhibit correlation with the original at specific intervals (time lags). When the delay increases, assuming the excitation is random, the correlation is expected to diminish progressively towards zero. While an ACF identifies the periodicities shared between the two signals, an CCF compares the delayed signal to a reference signal, extracting the common periodicities to signals from two different measurement locations.

These correlation functions are transformed in frequency domain via the Discrete Fourier Transform, generating the correlograms or power spectra. Diving the functions used to acquire the original data by the frequency resolution δf, it is possible to produce the cross-power spectral densities (CPSD) and auto-power spectral densities (APSD) (Center, S.S., 2020a).

With both methods, and the respective functions calculated, it is possible to compute the stabilization diagram with resource to a modal parameter estimator method, to obtain the modal parameters of the physical modes.

2.1.4. Modal Assurance Criterion

The Modal Assurance Criterion (MAC) is a popular tool to compare modal vectors in a quantitative way (Allemang, R.J., 2003). This criterion was developed after the development of the ordinary coherence calculation associated with the computation of the frequency response functions. The MAC and the ordinary coherence are statistical indicators. This least squares-based form a linear regression analysis yields an indicator that is more sensitive to the largest difference between comparative values and results in modal assurance criterion, than to small changes or small magnitudes.

Initially this parameter was introduced with The Modal Scale Factor in modal testing, as an additional confidence factor for the evaluation of the modal vector in different excitation locations. When an FRF is represented using the partial fraction expansion form, each term's numerator corresponds to the matrix of residues or modal constants.

The MAC is determined as a scalar product of the two sets of vectors $\{\boldsymbol{\Psi}_A\}$ and $\{\boldsymbol{\Psi}_X\}$, being organized into the MAC matrix presented in equation (2.9).

$$MAC(r,q) = \frac{|\{\boldsymbol{\Psi_A}\}_r^T\{\boldsymbol{\Psi_X}\}_s|^2}{(\{\boldsymbol{\Psi_A}\}_r^T\{\boldsymbol{\Psi_A}\}_s)(\{\boldsymbol{\Psi_X}\}_r^T\{\boldsymbol{\Psi_X}\}_s)} \tag{2.9}$$

Where it is possible to recognize the form of the coherence function, indicating the relation between $\{\boldsymbol{\Psi_A}\}$ and $\{\boldsymbol{\Psi_X}\}$.

In this case the modulus in the numerator is taken after the vector multiplication, so that the absolute value of the sum of product elements is squared. One equivalent formulation is showed in equation (2.10).

$$MAC(A,X) = \frac{|\sum_{j=1}^{n}\{\boldsymbol{\Psi_A}\}_j\{\boldsymbol{\Psi_X}\}_j|}{(\sum_{j=1}^{n}\{\boldsymbol{\Psi_A}\}_j^2)(\sum_{j=1}^{n}\{\boldsymbol{\Psi_X}\}_j^2)} \tag{2.10}$$

This criterion has been used as a Mode Shape Correlation Constant to quantify the accuracy of identified mode shapes. For complex modes of vibration, the MAC can be calculated as demonstrated in equation (2.11), where is clearly a real quantity, even if the mode shape data are complex.

$$MAC(r,q) = \frac{|\{\boldsymbol{\Psi_A}\}_r^T\{\boldsymbol{\Psi_X}\}_q^*|^2}{(\{\boldsymbol{\Psi_A}\}_r^T\{\boldsymbol{\Psi_A}\}_q^*)(\{\boldsymbol{\Psi_X}\}_r^T\{\boldsymbol{\Psi_X}\}_q^*)} \tag{2.11}$$

The MAC takes values between 0 and 1 when there is no consistent correspondence or the opposite, respectively. Values higher than 0.9 represent consistent correspondence while small values are an indicator of poor resemblance between the two mode shapes (Pastor, M. [et al.], 2012).

2.2. Density-Based Spatial Clustering of Applications with Noise

The Density-Based Spatial Clustering of Applications with Noise (DBSCAN) algorithm forms clusters by delineating various density regions. Unlike many other clustering techniques that demand a predefined number of clusters, DBSCAN relies on two input parameters: the radius ε and the minimum number of points that should fall within this radius (Ester, M. [et al.], 1996).

In Figure 2.5 are presented the main principles of the methodology. The core point (shown in blue) described by the hyperparameters mentioned above is easily identifiable. It represents the starting point of a cluster, containing within its radius the minimum number of points required to form a cluster. Additionally, any point falling within this radius is automatically included in the cluster. If the added points meet all the conditions to be considered core points, the procedure is repeated. However, if the added points do not fulfil the criteria to be core points, they will be designated as border points (black). Points that fail to meet the criteria for core or border points will be classified as noise and will not be assigned to any cluster (red) (Tavares, A. [et al.], 2023).

This method will be explained with more detail further on, in section 3.1.1.

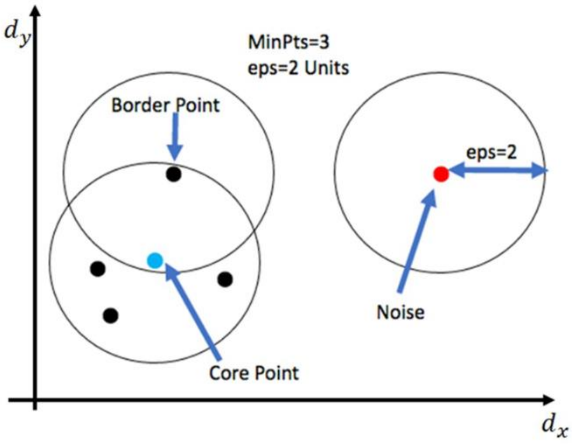

Figure 2.5 - Principles of DBSCAN (Tavares, A. [et al.], 2023).

3

AUTOMATED MODAL ANALYSIS METHODOLOGY

3.1. Automated Modal Parameter Selection

The Automated Modal Parameter Selection (AMPS) methodology is presented in Figure 3.1. This methodology is composed by three steps. First, it creates the clusters based in the poles represented on the stabilization diagram, taking as input the modal parameters estimated. A density-based clustering algorithm, DBSCAN, is employed for this purpose. This technique also discards some poles classified as noise in the initial process. Afterwards, the resonance modes identified by the clustering methodology undergo for two verifications steps. First, due to the complexity of some structures, is assured that all the modes are not split in two or more clusters in case they meet some conditions. Finally, the second verification step aims to identify and eliminate any potential spurious or numerical modes by analysing the characteristics of the clusters and their contributions to the final FRF synthesis (Tavares, A. [et al.], 2024). In the next sections, there will be a more detailed explanation of the steps of this AMPS methodology.

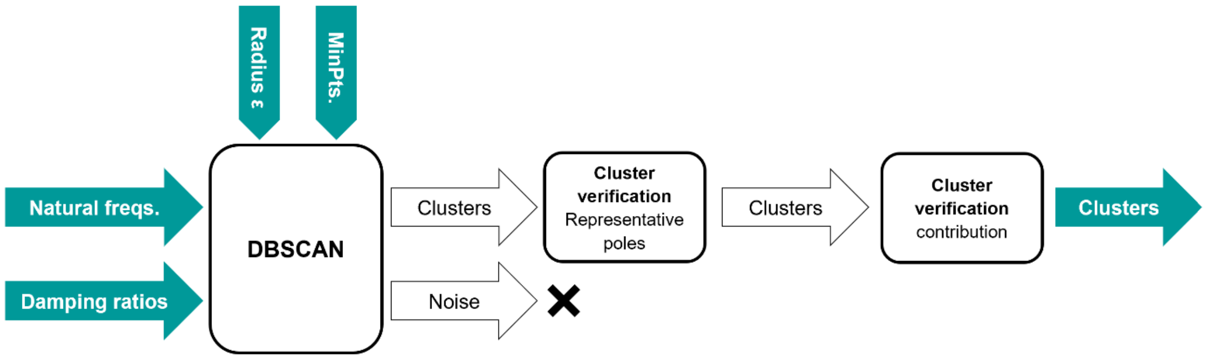

Figure 3.1 - Methodology for Automated Modal Parameter Selection (AMPS) (Tavares, A. [et al.], 2023).

3.1.1. DBSCAN Clustering Technique

Utilising the natural frequencies and damping ratios as inputs, it becomes possible to build the initial clusters of poles on a stabilization diagram with recourse to DBSCAN. An important step in the clustering process is the computation of the distance between poles, that is adjusted to the modal parameters considered as input. This distance is calculated by the sum of the absolute differences in normalized frequency and damping, owing to the different magnitudes and units of the two inputs. The formulation to calculate the distance is presented in equation (3.1), where the variables have the next denotation: p_i, p_j are the pole-i and pole-j, respectively, and N_p is the number of poles in the stabilization diagram.

$$d(p_i) = d_f(p_i) + d_\xi(p_i) = \frac{|f_{p_i} - f_{p_j}|}{f_{p_i}} + \frac{|\xi_{p_i} - \xi_{p_j}|}{\xi_{p_i}} \; ; i,j \; \in \{1,2,\ldots,N_p\} \tag{3.1}$$

To guarantee the versatility of the AMPS methodology implemented to diverse structure's stabilization diagram with different characteristics, such as modal densities and model sizes, the DBSCAN has meticulously chosen hyperparameters. As hyperparameter the methodology has the minimum number of points (*MinPts*), that is one-sixteenth (1/16) of the model size, having a lower limit of 3. For DBSCAN is also defined the epsilon distance (ε), that takes 0.06 as a value established in agreement with the tolerances for the natural frequency and damping ratio that define a stable pole in the stabilization diagram (1% for frequency and 5% for damping (Lau, J. [et al.], 2007)) (Tavares, A. [et al.], 2024).

3.1.2. First Verification Step

This verification step, focusing on the representative poles of each cluster, aims to ensure that single modes are not split. Based on the closeness to the median frequency and damping inside the cluster, the representative pole is selected. When analysing stabilization diagrams computed with high model orders, like for complex structures as fully equipped cars or airplanes, this step is crucial. In some situations, significant discrepancies in the damping ratios of poles calculated for the same mode often occur, enhancing the formation of multiple clusters.

To make the verification, are identified the secondary clusters to associate to the primary ones, excluding them, at the same time, from the representative pole selection. To execute this, two distance metrics are computed between the representative poles (rp) of the number of clusters (N_c), and then the next clustering phases are performed: a) frequency distance, equation (3.2) and b) the MAC distance among the modal participation factors (L), equation (3.3). In the case of this distances present a value below 2% and 20%, respectively, the clusters can be linked and fused if they met some conditions, according with the scheme presented in Figure 3.2 (Tavares, A. [et al.], 2024).

$$d_f(rp_i) = \frac{|f_{rp_i} - f_{rp_j}|}{f_{rp_i}}; \; i,j \; \in \; \{1,2,\ldots,N_p\} \tag{3.2}$$

$$d_{MAC(L)}(rp_i) = 1 - \frac{\left|L_{rp_i} L_{rp_j}\right|^2}{\left(L_{rp_i} L_{rp_i}\right)\left(L_{rp_j} L_{rp_j}\right)}; \; i,j \; \in \; \{1,2,\ldots,N_p\} \tag{3.3}$$

Some structures, such as wind turbines (Oliveira, G. [et al.], 2018), exhibit complex structural dynamics that result in multiple physical modes occurring at very close frequencies. Therefore, for the initial verification step, with the structure shown in Figure 3.2 was employed to determine whether the secondary mode should be merged with the primary cluster.

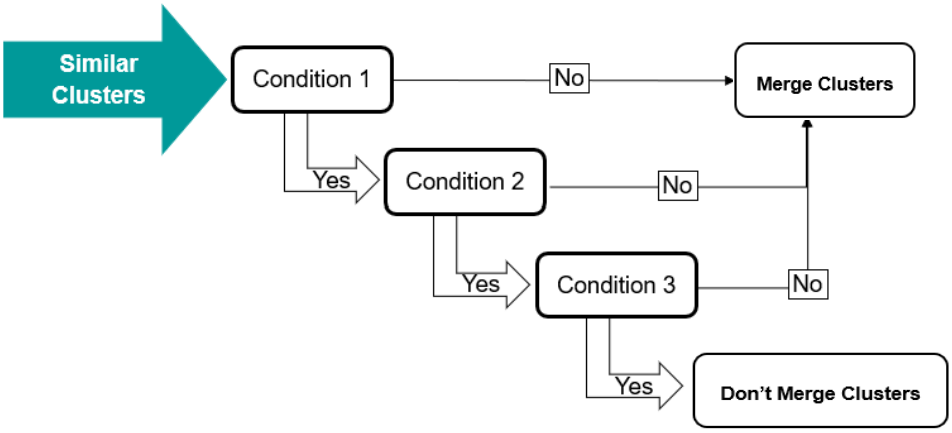

Figure 3.2 - First Verification Step.

The conditions, presented in Figure 3.2 - First Verification Step, to be fulfilled are the following:

1. The secondary cluster must have, at least, 50% the number of poles of the primary one.
2. To pass to the condition number 3, the clusters should have a coincidence of the modal orders.
3. The clusters must have a coincidence of poles at the same model order, no less than 50%.

3.1.3. Second Verification Step

To find and remove potential numerical modes, the second verification step analyses the impact of modes after the first verification step, on the ultimate mode set and the FRF synthesis. Numerical modes can appear due to some reasons, such as over-selection of the model order for the computation of the stabilization diagram, measurement-related problems, or even a combination of the two. The over-selection of model order to the model parameter estimator (MPE) will affect a proper fitting of the high-order polynomial to the data, what can tease a sensibility to small dynamics on the data that are not triggered by the physical resonant behaviour of the structure. Also, the measurement problems can produce noise in the response data, which will generate spurious poles in the stabilization diagram during the fits of the MPE to the modal model data (Tavares, A. [et al.], 2024).

An in-house method was applied to calculate the contribution of the modes with respect to the modal model synthesis. The contribution of a mode is associated to the representative pole of its cluster (Tavares, A. [et al.], 2024).

To remove the potential numerical modes, classified as dubious by the method, the clusters must meet the conditions explained in Figure 3.3. Before the classification of each cluster, the reference modes are selected based on the representative poles that contribute the most to the frequency-domain response. Afterwards, are defined quantities like the minimum reference contribution (*minRef_contribution)*, the maximum damping ratio and the minimum number of poles within the reference clusters. There are also set some important values, such as the limit contribution to start doubting about a cluster (*limDubPolCheck*), 0.02, and the fraction of poles that a cluster must have to be classified as a physical cluster (*difPolesRef*), 85%, compared with the minimum number of poles of the reference modeset.

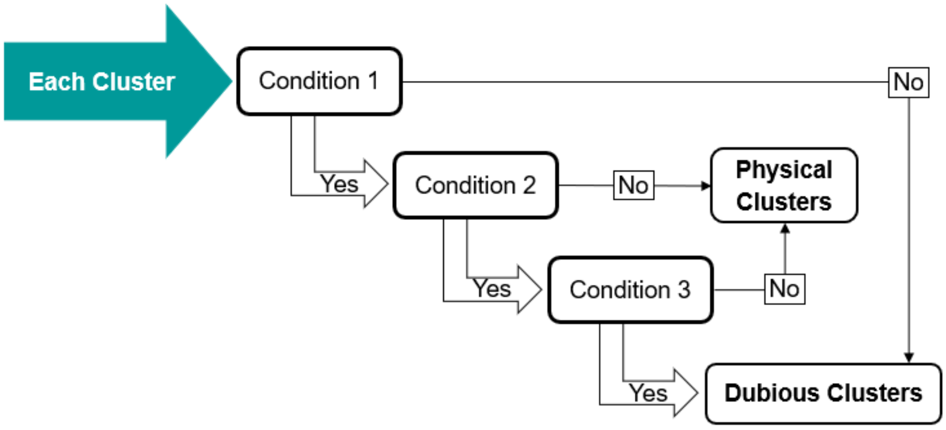

Figure 3.3 - Second Step Verification.

Following the process referred above, the cluster are submitted to the next conditions:

1. The damping of the cluster in analysis should not exceed ten times the maximum reference damping, otherwise it will be considered a dubious cluster.
2. To proceed to the next condition, the cluster contribution must be lower than the minimum contribution allowed. This value can take two different values, if the *minRef_contribution* is higher than the *limDubPolCheck*, the minimum contribution allowed is the *minRef_contribution* minus 0.01, or if the condition is not verified, it will take has value half of the *minRef_contribution*.
3. The final condition that a cluster should meet, to be considered dubious, is related to the number of poles. If the cluster does not have the *difPolesRef* of the minimum reference number of poles or at least have less than the double of the *MinPts*, then the cluster will be classified as dubious.

3.2. Automated Modal Tracking

The modal tracking technique assesses the resemblance between the modal parameters obtained from a particular measurement and a predetermined set of reference modes across time. In essence, modal tracking monitors the evolution of modal parameters over time, leveraging correlations established through this process.

In Figure 3.4 is summarized all the process adopted to the automated modal analysis (AMA), where is possible to see that the modal tracking is preceded by two steps, first, the modal parameter estimation (MPE) and then an automated modal parameter selection (AMPS). The first step involves using PolyMax, as described in subsection 2.1.2, to calculate the modal parameters of all poles and plot them in a stabilization diagram, being feasible to execute in a context of EMA or OMA (present in subsection 2.1.3). The AMPS step focuses on accessing the final resonance modes through the stabilization diagram and the corresponding set of poles to characterize the dynamic behaviour of the structure. In the present work, this step is performed by the methodology defined in section 3.1. Modal tracking permits the study over multiple measurements to track a set of reference modes over time (Devriendt, C. [et al.], 2014).

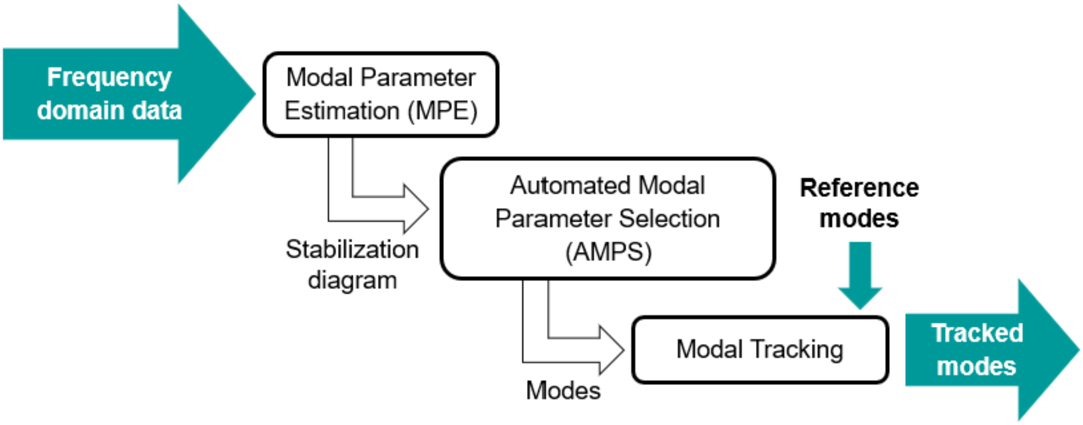

Figure 3.4 - Automated Modal Analysis (AMA) Process.

To perform the tracking of the resonance modes is calculated the distance between the modal parameters and, if this value drops below a certain threshold is established a similarity between modes. In the present work, the modal parameters evaluated are natural frequencies and mode shapes in agreement with the equations (3.4) and (3.5). Taking into account the two modal parameters referred before, and considering a mode 1 (m_1) as a set of modes calculated for one measurement, and a mode 2 (m_2) from a set reference modes to be tracked time, it is possible to establish a correlation between mode 1 and mode 2 in terms of frequency distance (equation (3.4)) and MAC distance (equation (3.5)) if this values are both above a defined threshold. These thresholds are defined depending on the application in study, because every structure has a specific behaviour. The MAC distance is the more affected by this statement, because it can vary considerably depending on the number of Degrees-of-Freedom (DOF) in analysis.

$$d_{freq} = \frac{|f_{m_1} - f_{m_2}|}{f_{m_1}} \tag{3.4}$$

$$d_{MAC} = 1 - \frac{|\phi_{m_1}\phi_{m_2}|^2}{(\phi_{m_1}\phi_{m_1})(\phi_{m_2}\phi_{m_2})} \tag{3.5}$$

4

VALIDATION FOR INDUSTRIAL DATASETS

4.1. Industrial Datasets Description

To validate the proposed methodology, presented in section 3.1, 8 experimental industrial datasets were used. These datasets are presented in Figure 4.1.

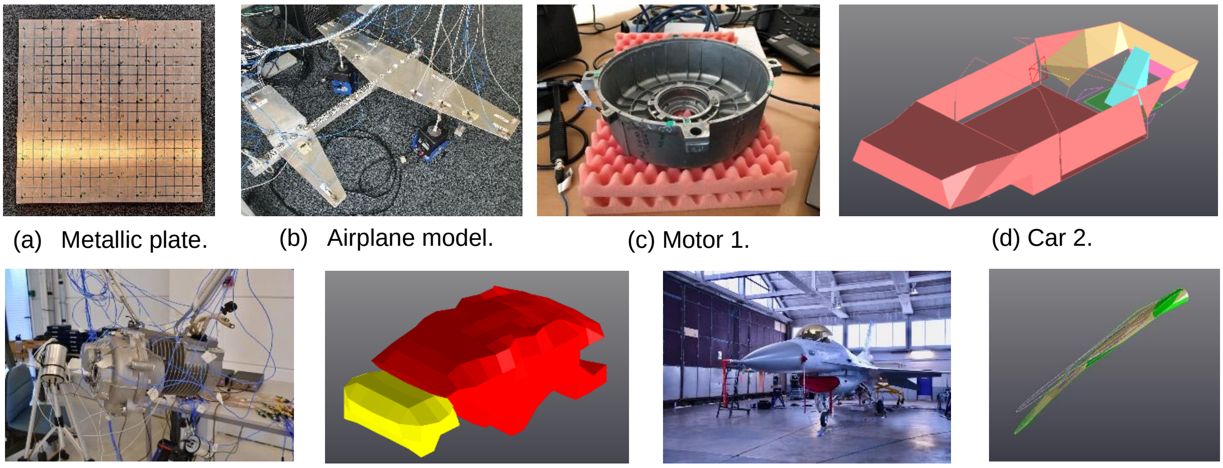

(a) Metallic plate. (b) Airplane model. (c) Motor 1. (d) Car 2.

(e) Motor 2. (f) Car 1. (g) F16 jet. (e) Wind Turbine Blade.

Figure 4.1 - Images of the datasets used to validate the AMPS methodology (Tavares, A. [et al.], 2024).

The metallic plate (Figure 4.1a) has a symmetrical square shape with a side length of 400 mm. The plate was suspended to simulate free-free boundary conditions and was excited at two points using a modal hammer. Fifteen uni-axial accelerometers were used to measure the plate’s acceleration response. For the airplane model (Figure 4.1b), which measures 733 mm in length and 914 mm in wingspan, sixteen accelerometers were utilized: thirteen uni-axial and three tri-axial, providing the excitation with two modal shakers positioned under each wing, delivering a pseudo-random excitation signal. The measurements in F16 fighter jet (Figure 4.1g), with a length of approximately 15 m and a wingspan of 10 m, were done while it was positioned in the hangar. To proceed to the measurement, the dataset included thirty-five tri-axial accelerometers placed in various points on the aircraft, such as the fuselage, wings, flaps, tails, fin, and payloads. To excite the structure with a pseudo-random signal, two modal shakers were positioned below the wings.

The remaining datasets, presented in Figure 4.1, such as, the two motors, the two fully trimmed cars and the wind turbine blade, present a wide range of different characteristics, like various types of sensor measurements (acoustic microphones, uni and tri-axial accelerometers), types of excitations (impact, shaker, and Qsource testing), and frequency bands under consideration spanning from below 50Hz to over 4000 Hz. The structures presented in Table 4.1 vary significantly in size, complexity, and application, ranging from a small symmetrical plate to fully trimmed cars and airplanes. In the same table, it is possible to see a summarized overview of all the measurement setups and all the detail aspects, like number of sensors, type of excitation and frequency band of interest (Tavares, A. [et al.], 2024).

Table 4.1 - Information of the datasets used for validating the second step verification (Tavares, A. [et al.], 2024).

Name	Description	Data acquisition	Excitation	Frequency Band	Difficulty
Metallic plate	Symmetric metallic plate	15 uni-axial accelerometers	Modal hammer (2 locations)	[20, 930] Hz	2/5
Airplane model	Airplane metallic structure	13 uni-axial + 3 tri-axial accelerometers	Modal shaker (2 shakers)	[0, 400] Hz	2/5
F16 jet	Ground Vibration Testing (GVT) to F16 fighter jet aircraft	35 tri-axial accelerometers	Modal shaker (2 shakers)	[1.1, 45] Hz	4/5
Wind turbine blade	Titanium wind turbine blade frame	10 tri-axial accelerometers	Modal hammer (1 location)	[0, 800] Hz	2/5
Motor 1	Casing from industrial electric motor	2 uni-axial accelerometers	Modal shaker (2 shakers)	[400, 4100] Hz	3/5
Motor 2	Gearbox from convertible car	Roving tri-axial accelerometers (30 locations)	Modal shaker (2 shakers)	[200, 3330] Hz	5/5
Car 1	Acoustic measurement to fully trimmed sedan car	34 microphones	Q-MED qsource exciter (12 locations)	[30, 550] Hz	4/5
Car 2	American convertible car	125 tri-axial accelerometers	Modal shaker (2 shakers)	[1.2, 45] Hz	5/5

4.2. RESULTS

To better comprehend the influence of the second verification step of the AMPS process, presented in chapter 3, on the stabilization diagram produced with PolyMax (subsection 2.1.2), there were considered 3 structures as baseline to the analysis. The structures are the metallic plate (Figure 4.1a), the airplane model (Figure 4.1b) and the F16 jet (Figure 4.1g). The 3 structures will be analysed with some detail in the present section, as it was done in (Tavares, A. [et al.], 2024).

In the three cases, first is presented the "(a) Stabilization Diagram", which represents the original stabilization diagram, before the AMPS methodology is applied to the data presented in the diagram, presenting the stabilization diagram generated by PolyMax (subsection 2.1.2). In this diagram every blue point represents a stable pole, and the red curve the sum of the measured FRFs. Then is presented "(b) After AMPS methodology", with the stabilization diagram affected by the AMPS methodology. This stabilization diagram has poles classified as -2, -1 and positive values. The classified as -2, are the spurious clusters identified and eliminated by the second verification step of the AMPS methodology (subsection 3.1.3). The -1 represent the noise points detected by the DBSCAN (subsection 3.1.1), and the positive values characterize the clusters formed by the AMPS methodology (section 3.1), where the pink crosses identify the representative pole chosen for each mode.

First, is displayed in Figure 4.2, the results to the metallic plate. Some of the values considered to this analysis and some specifications of the test performed, principally the frequency band, are already presented on Table 4.1. It was, also considered a model order of 88 for the analysis, with the purpose of showing the accuracy of the method on eliminating the spurious modes, as is possible to see in Figure 4.2b. For the analysis of this structure, and only to do the identification of the physical modes it was not needed to set a high model order as in this case, it was adopted that value due to the reason already explained.

The columns of poles associated to the main resonance peaks are clear, well defined, and the method does not eliminate them. Whereas the others, like the ones presented in frequencies around 100 Hz, 350 Hz, 460Hz and 500Hz, with a smaller representation in the diagram that clearly does not represent a physical mode, are eliminated, and classified as -2. There are two clusters that presents a very marked presence in the stabilization diagram, with a frequency approximated to 700 Hz, and even in this case, clusters were eliminated by the method, representing a positive aspect, since these two are not related to a peak of the FRF sum represented.

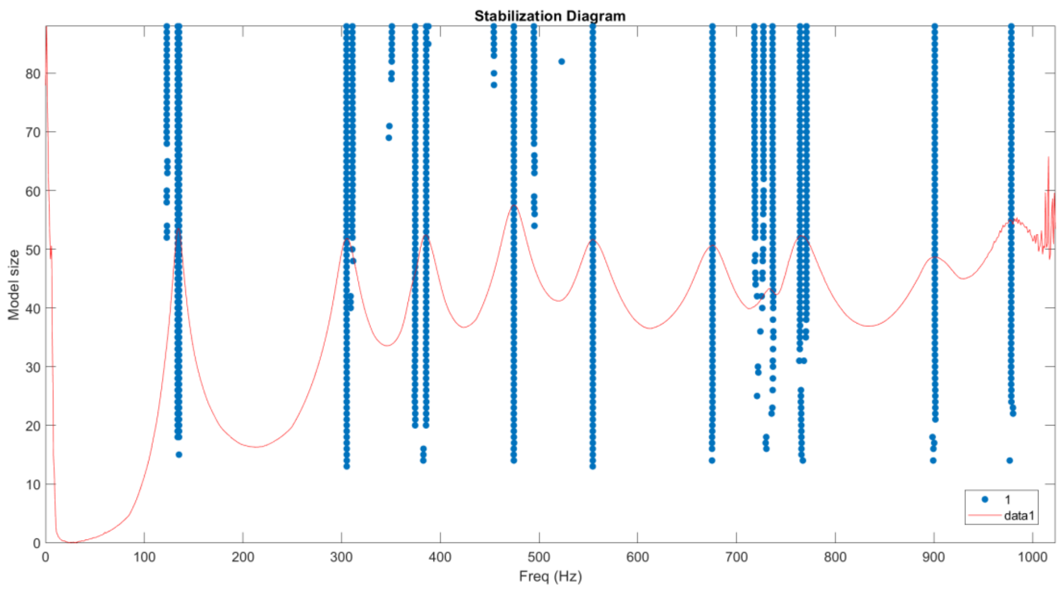

(a) Stabilization Diagram.

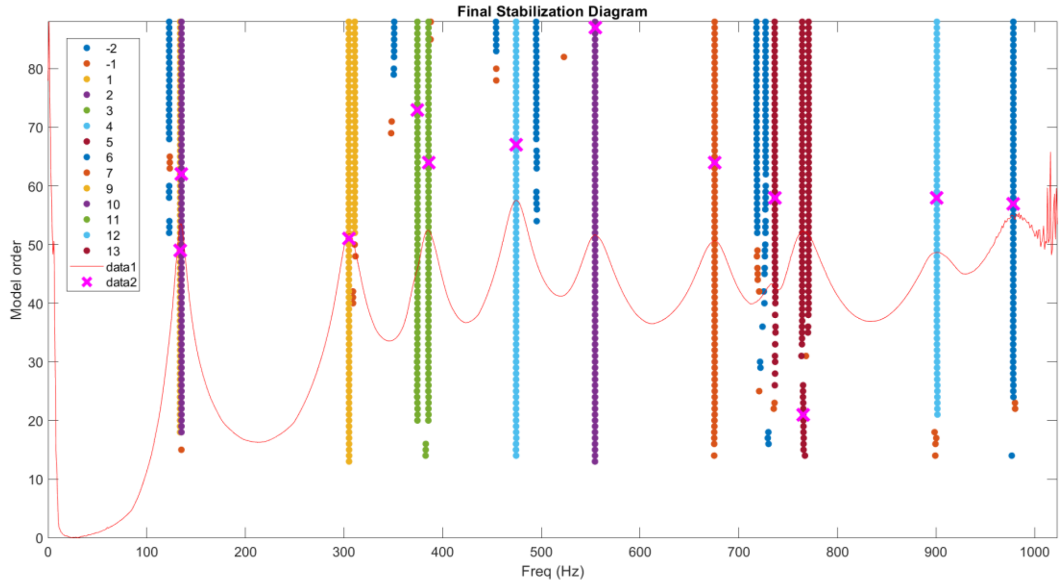

(b) After AMPS methodology.

Figure 4.2 - AMPS results for the metallic plate.

The results of the airplane model (Figure 4.3) were obtained to a model order of 80. It was considered a frequency band of [0, 400] Hz and 2 inputs (shakers). As in the case of the metallic plate (Figure 4.2), is clear the difference between the physical resonance modes and the numerical ones. It is possible to find the numerical clusters (-2) in the frequency band [200,350] Hz. Other characteristics of the test perform to this dataset can be found in Table 4.1.

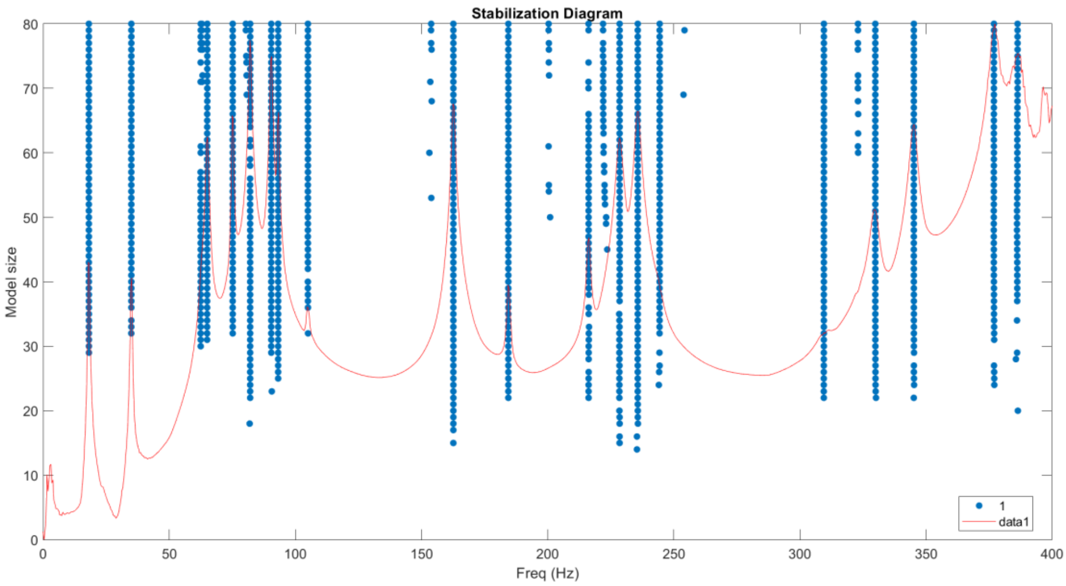

(a) Stabilization Diagram.

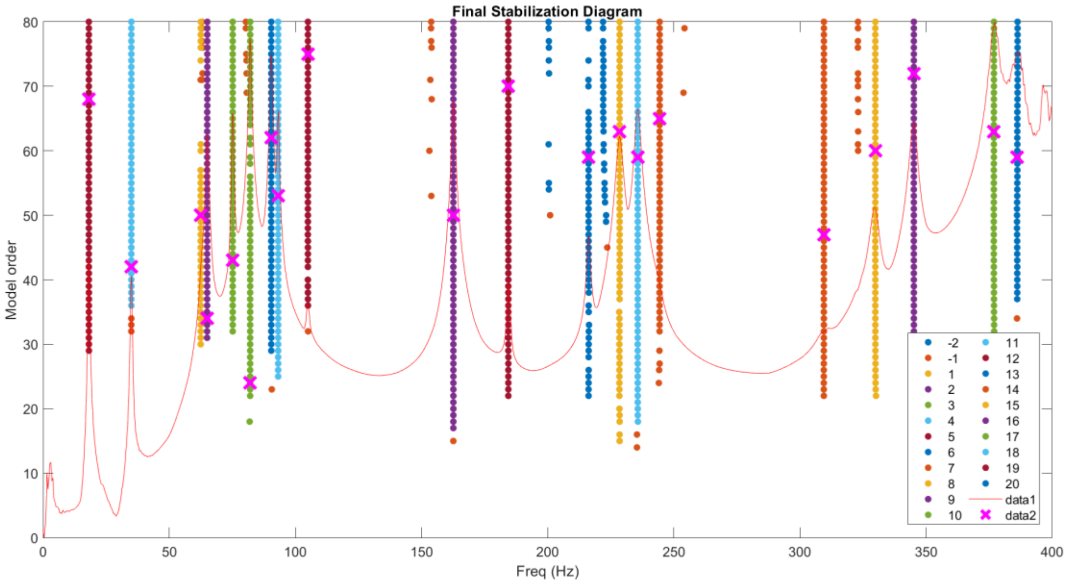

(b) After AMPS methodology.

Figure 4.3 - AMPS results for the Airplane Model.

This last structure, the F16 jet dataset for a frequency interval [1.2,45] Hz, one of the more complex datasets, considering the 2 inputs (shakers) and a model size of 100, with the AMPS methodology two spurious modes were identified, one around a frequency of 3 Hz and another one nearby the 15 Hz (Figure 4.4). The remaining modes are correctly clustered as resonance modes, as in the other examples. In Table 4.1 are presented the details of the test performed to this structure.

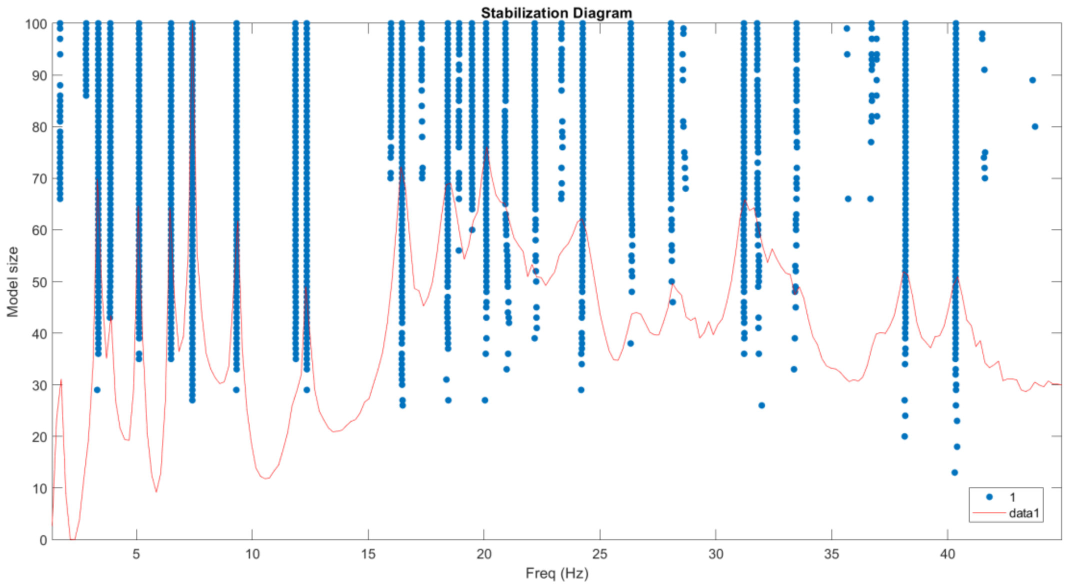

(a) Stabilization Diagram.

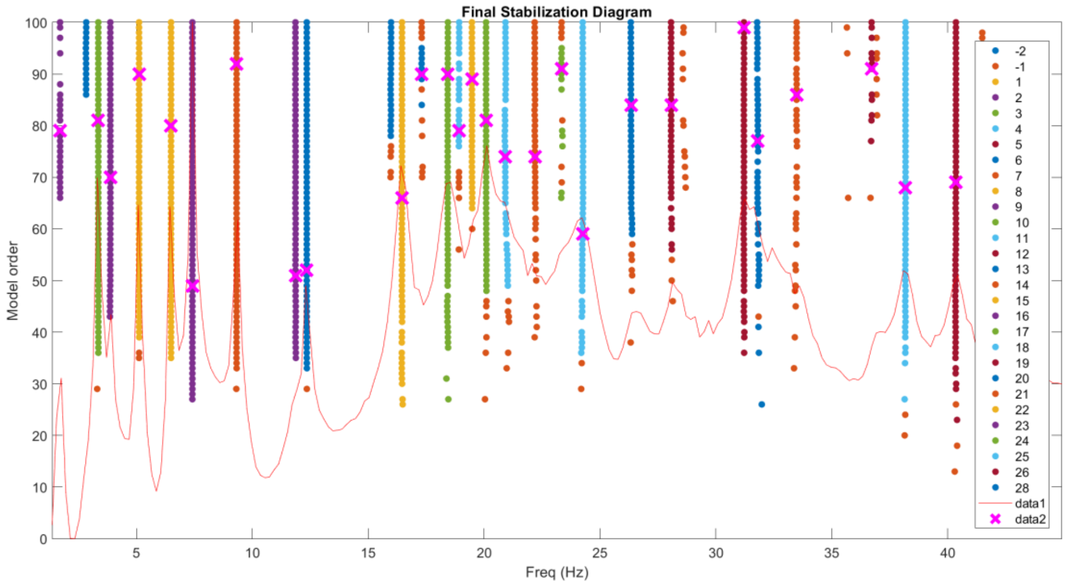

(b) After AMPS methodology.

Figure 4.4 - AMPS results for the F16 jet.

The remaining structures were also analysed, yielding similarly positive results as those shown in Figure 4.2, Figure 4.3 and Figure 4.4.

The processing time of the AMPS methodology was also recorded for the calculation of the eight datasets. The minimum time, approximately 0.04 second, was obtained for the wind turbine blade, while the maximum time, around 0.7 seconds, was recorded for Motor 1.

4.3. Benchmark Validation

To better understand the performance of the AMPS methodology proposed in section 3.1, a benchmark study was performed based in the eight industrial datasets presented in section 4.1. The benchmark study counted with a participation of multiple engineers of different expertise levels.

When structures are subjected to challenging experimental setups in the modal analysis domain, establishing a ground-truth modal selection for a given dataset can be demanding. The alignment between real-world testing and ideal scenarios is often not possible. Characteristics such as fully free-free or fully fixed boundary conditions can interfere with the interaction between the excitation and the structure, potentially introducing additional dynamics into the measured data. Therefore, in the stabilization diagram, modes resulting from the interaction between the structure and these imperfect boundary conditions may be present. The relevance of this modes always depends on the engineer judgment, and the diverse goals that he might have in modal analysis of a specific structure (Tavares, A. [et al.], 2024).

The jury test conducted for this benchmark study included 24 engineers distributed equally across three expertise levels, as shown in Table 4.2. To categorize the engineers into the corresponding expertise levels, several factors were taken into consideration, such as the number of datasets analysed, years of experience, and the frequency with which they work with modal analysis. Level 1 represents a participant who engages in modal analysis with lower regularity but has a general understanding of the concepts. They could be an NVH researcher who performs modal analysis yearly and has some experience analysing 10 to 20 datasets, even though it is not their main area of expertise. In Level 2, participants typically conduct modal analysis monthly and have experience with 20 to 60 datasets. They demonstrate a higher level of expertise and may include PhD researchers or customer support engineers specializing in structural dynamics testing. In Level 3, participants often hold roles such as product managers or research managers in structural dynamics, demonstrating a high level of expertise with a strong focus on modal analysis. They typically have more than fifteen years of knowledge and experience, having analysed more than 60 datasets (Tavares, A. [et al.], 2024).

The participants also rated the difficulty level of each dataset on a scale from one to five, with one indicating a very low difficulty and five the high difficulty. The score for each dataset is presented in Table 4.1.

The results for the three expertise levels mentioned afterwards are derived from a recent study (Tavares, A. [et al.], 2024), in which the same benchmark study was conducted using different AMPS methodologies.

Table 4.2 - User levels of the participants in the jury test (Tavares, A. [et al.], 2024).

Level	Description	Number of users
1	Novice user: general knowledge of modal analysis Less frequent user	8
2	Intermediate user: good knowledge of modal analysis Periodic user	8
3	Expert user: very good knowledge of modal analysis Daily User	8

To draw conclusions about the benchmark validation, four different metrics were analysed: the number of selected modes, the FRF synthesis error, the number of modes correlated with the expert users (Level 3), and the number of modes uncorrelated with the expert users.

4.3.1. Number of Modes

As mentioned earlier in this section, one of the most challenging tasks in the field of modal analysis is the identification of modes for complex datasets by engineers with less experience. Figure 4.5 illustrates the average number of modes selected by the various expertise levels and the AMPS methodology under analysis, over the eight different datasets.

By analysing Figure 4.5, a notable difference is evident in the number of modes identified by experts at level one compared to those at level three, particularly in complex datasets such as 'Car 1 and 2', 'Motor 2', and 'F16 jet'. Overall, expert users (level 3) tend to select a higher number of modes, averaging around

183 modes across all datasets. Intermediate users (level 2) selected approximately 160 modes, whereas novice users (level 1) opted for a lower number of modes, averaging around 133.

Considering the AMPS methodology (DBSCAN), it identified approximately 182 modes across all datasets. Generally, there is a degree of consistency and proximity between the number of modes selected by expert users (level 3) and this methodology.

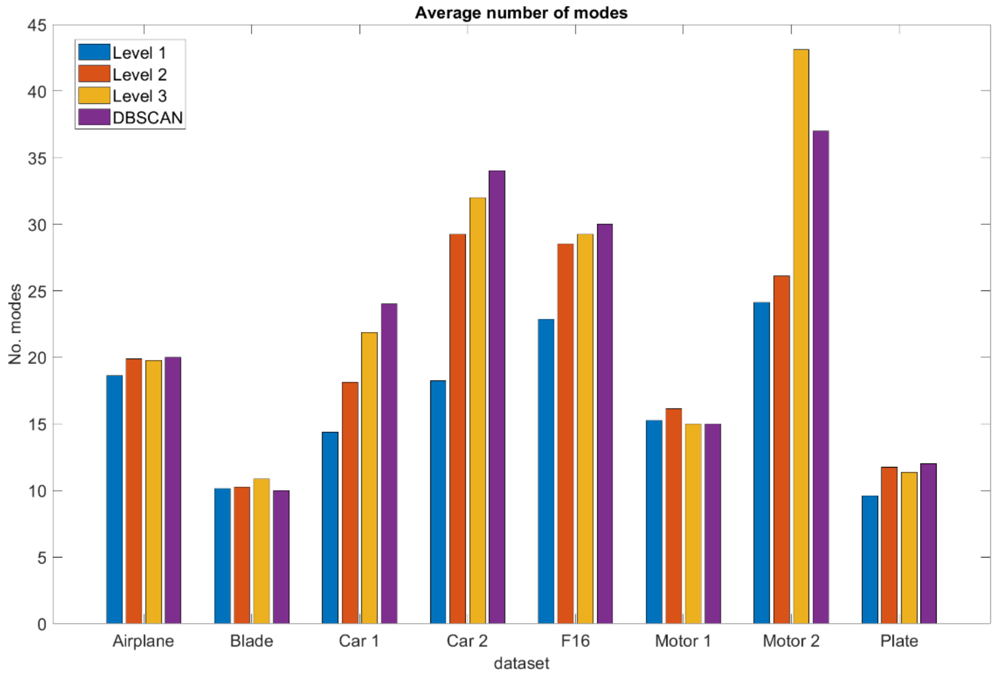

Figure 4.5 - Number of modes identified for the eight datasets by the participants of the different levels and the AMPS methodology (DBSCAN).

4.3.2. FRF Synthesis Error

To evaluate the quality of the modesets selected by the different participants or by the AMPS methodology, the error between the synthesis FRF (H^s) using the chosen modeset M, and the measured FRF (H^m) can be analysed. The FRF synthesis is derived by the modal model equation (equation (2.1)) based on the modal parameters of the selected poles in the modeset M. The evaluation of this parameter (H_{error}) permits to analyse how well the chosen modes represent the structure's dynamics compared to the measured data. With this information, the user can determine whether the modal model accurately captures all the important resonance peaks or if extra modes were included. It is possible to assess whether the selection of extra modes represents the missing dynamics or if it corresponds to the inclusion of numerical poles related to noise in the measured response.

The analysis of the FRF synthesis error (H_{error}) presented in equation (4.1) aims to evaluate the capability of selecting poles on a stabilization diagram that closely represent the structure's dynamics. By comparing the errors across different types of users and the AMPS methodology, the focus is on this correspondence, as there are always differences between the experimental data and the modal model. Therefore, achieving a zero FRF synthesis error is not expected, but a lower value indicates a good selection of the poles (Tavares, A. [et al.], 2024).

$$H_{error}(M) = \frac{\|H^m - H^s(M)\|_1}{\|H^m\|_1} \tag{4.1}$$

Figure 4.6 presents the average FRF synthesis error for the three user levels and the adopted AMPS methodology. Generally, the FRF synthesis error increases from the expert users (Level 3) to the intermediate users (Level 2) and reaches the highest level in the novice users (Level 1). This trend clearly reflects the improvement in modal selection with increasing user expertise. It is also notable that novice users have increased difficulty in selecting the modes on the stabilization diagram, particularly when dealing with more complex structures such as the two cars, the F16 jet, and Motor 2.

The AMPS methodology generally achieves lower FRF synthesis error values than those obtained by all user levels. This demonstrates the accuracy of the methodology in identifying modes related to the structure's dynamics.

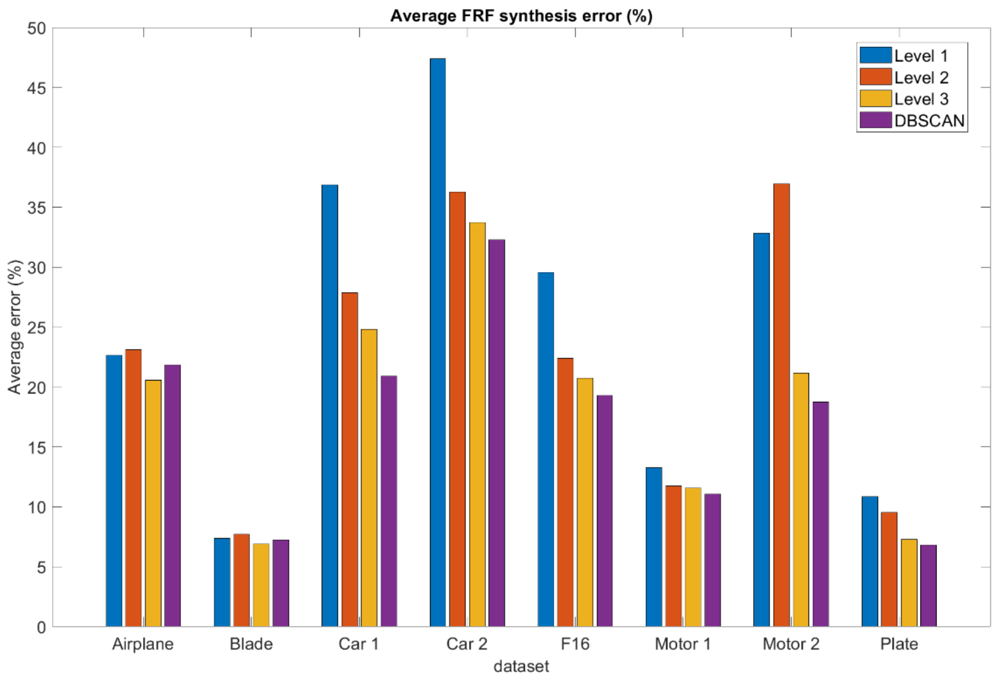

Figure 4.6 - FRF synthesis for the eight datasets by the participants of the different levels and the AMPS methodology (DBSCAN).

4.3.3. Number of modes correlated with expert users

Assessing the number of modes and the FRF synthesis error, it is important to understand how the results obtained by the novice and intermediate levels, as well as the AMPS methodology, align with the choices of the experts (Level 3). Although the FRF synthesis error indicates how well the selected modeset represents a system's dynamics, it is crucial to compare these results with the expert selections to ensure consistency and accuracy. The main objective of this comparison is to determine whether the selected modes correspond to the resonant modes or if they are merely numerical modes caused by noise in the response data, which could lead to a higher FRF synthesis error. To achieve this, the modes selected by the users and the DBSCAN method are compared with those chosen by the expert group (Level 3). This comparison involves calculating a frequency distance (d_{freq}) under 2% and a MAC distance (d_{MAC}) below 40%, as represented in equations (3.4) and (3.5) (Tavares, A. [et al.], 2024).

In Figure 4.7, the number of modes correlated with those selected by the expert users is displayed. On average, novice users exhibit a correspondence of 130 correlated modes, while intermediate users have 150 correlated modes. The AMPS methodology presents 181 correlated modes. Generally, DBSCAN offers a modeset more similar to that of the users than other levels of participants.

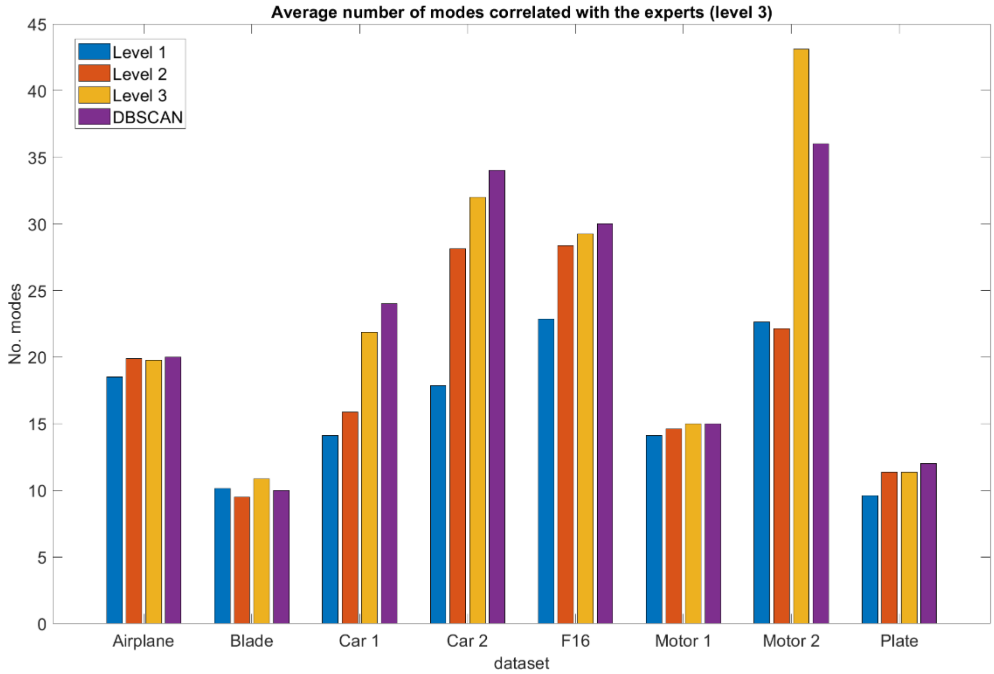

Figure 4.7 - Number of modes correlated to the experts' group (level 3) for the eight datasets by the participants of the different levels and the AMPS methodology (DBSCAN).

4.3.4. Number of modes uncorrelated with expert users

In Figure 4.8 is illustrated the difference between the total number of modes (Figure 4.5) and the ones correlated with the users level 3 (Figure 4.7) . This difference displayed in the figure can represent the potential numerical modes. Novice users (level 1) present only around 3 uncorrelated modes, in 5 of the 8 datasets, whereas the intermediate users (level 2), in average, selected 10 more modes on 7 different datasets. Although these results may seem counterintuitive due to the higher number of uncorrelated modes selected by intermediate users, the inexperience of novice users leads them to select fewer modes on the stabilization diagram. This results in fewer additional modes being included, but also in fewer physical modes being selected. Consequently, this leads to a higher FRF synthesis error, as demonstrated in subsection 4.3.2. When a low number of physical modes are selected, the modal models they represent are of inferior quality. (Tavares, A. [et al.], 2024).

The DBSCAN only presents one uncorrelated mode, for one of the datasets.

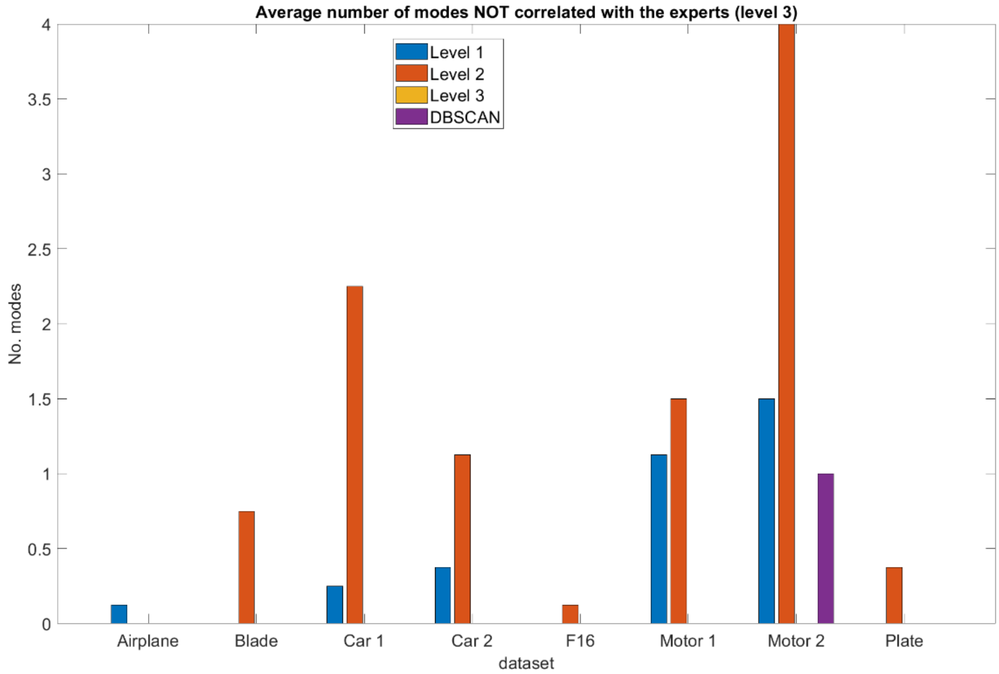

Figure 4.8 - Number of modes uncorrelated to the experts' group (level 3) for the eight datasets by the participants of the different levels and the AMPS methodology (DBSCAN).

4.3.5. Results Discussion

After evaluating the results of the benchmark validation, Table 4.3 presents a summary of all the outcomes, including the FRF synthesis error, number of selected modes, number of modes correlated with the experts, number of modes uncorrelated with the experts, and the number of datasets with selected uncorrelated modes (Tavares, A. [et al.], 2024).

The FRF synthesis error is greatest for novice users (Level 1), decreases for intermediate users (Level 2), and is even smaller for expert users (Level 3). Comparing this value with the AMPS methodology, it presents the lowest value of all.

In terms of the average number of selected modes, the expert users and the DBSCAN methodology show similarity in the number of modes selected. The novice users present the lowest value due to their inexperience in the field.

The number of uncorrelated modes initially seems suspicious because novice users have fewer uncorrelated modes than intermediate users. However, when this value is correlated with the FRF synthesis error, it becomes evident that novice users missed some physical modes, leading to a higher FRF synthesis error. The DBSCAN methodology had only one uncorrelated mode in one of the datasets, more specifically the 'motor 2'.

In summary, the DBSCAN methodology generally presents the lowest FRF synthesis error and the lowest number of uncorrelated modes, which supports the validity of the proposed methodology. Additionally, the calculation times for this methodology (subsection 4.2) are much faster than what can be achieved through manual selection by a user.

Table 4.3 - Sum of the results obtained for the metrics used to evaluate the benchmark study, for the eight datasets.

	Level 1	**Level 2**	**Level 3**	**DBSCAN**
FRF synthesis error (%)	200.77	175.49	146.74	138.15
Number of selected modes	133.25	160	183.25	182
Number of correlated modes	129.88	149.88	183.25	181
Number of uncorrelated modes	3.38	10.13	0	1
Number of datasets with uncorrelation	5/8	7/8	0	1/8

5
INFANTE DOM HENRIQUE BRIDGE MONITORING

5.1. Bridge Description

The Infante Dom Henrique Bridge is one of the several impressive works of art that spans the Douro River, linking the cities of Porto and Gaia, in the north of Portugal. Inaugurated in the beginning of the 21st century, this road bridge lies amidst two centenary metallic bridges, Maria Pia and Luiz I, and it is near to two concrete bridges of the 20th century, Arrábida and São João.

This concrete arch bridge, composed by two key interacting components: a highly rigid prestressed reinforced concrete box girder, 4.50m deep, supported by a very shallow and thin reinforced concrete arch, 1.50m thick, as is possible to see in the elevation and cross-sections in Figure 5.1. Between the abutments the arch spans 280m and rises 25m until the crown, presenting a shallowness ratio higher than 11/1. The arch and the deck meet up in the 70m central segments, defining a box-beam, 6m deep. The arch maintains a constant thickness, while its width gradually increases from 10 meters at the central span to 20 meters at the springs. The structure functions as a beam bridge defined between the abutments and the intermediate elastic supports 35m apart, due to the high stiffness of the deck compared with the slenderness of the arch (de Magalhães, F.M.R.L., 2010).

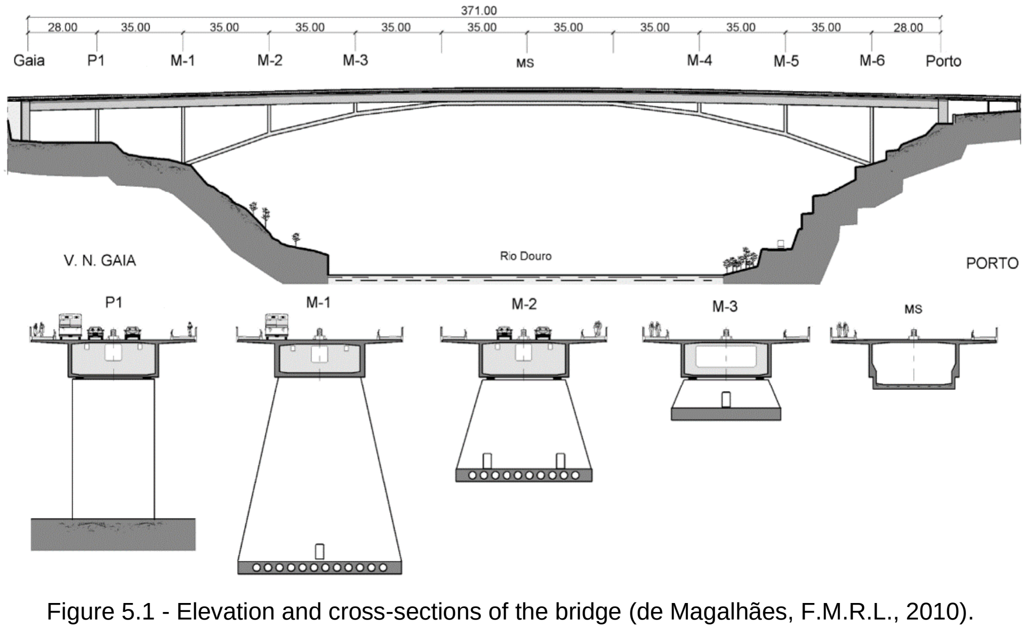

Figure 5.1 - Elevation and cross-sections of the bridge (de Magalhães, F.M.R.L., 2010).

An important aspect to keep in mind about the bridge is that it serves as one of the main entrances into the Porto city centre. This means it experiences a high volume of vehicle traffic, especially during morning and afternoon rush hours.

5.2. MONITORING SYSTEM DESCRIPTION

After the bridge construction, the dynamic monitoring of the bridge was done using 12 force balance accelerometers (Kinemetrics, Episensor), two digitizers (Kinemetrics, Q330) and corresponding recording units and an internet router. All the system was placed inside the box girder with the correspondent distribution present in Figure 5.2. It is possible to find a more detailed information of the hardware in (de Magalhães, F.M.R.L., 2010).

Because this monitoring system was later moved to another structure, a new replacement system was installed in 2018. In this case, it was adopted a customized system developed at FEUP. In addition to being significantly more affordable than the previous one, it works on batteries, avoiding the need to install cables throughout the structure.

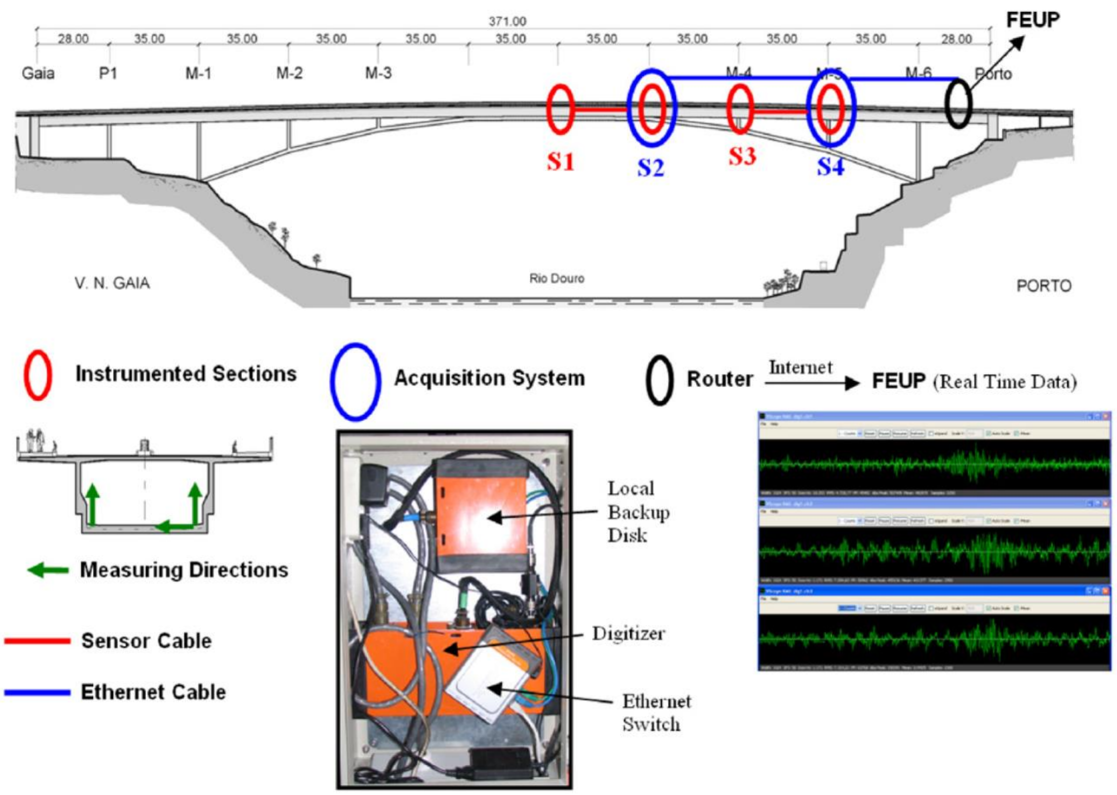

Figure 5.2 - Scheme of the monitoring system (Magalhães, F. [et al.], 2009)

Considering the previous work on the bridge, it is concluded that the use of 2 accelerometers was adequate for the long-term monitoring. As a result, 2 devices were installed in sections S2 and S4 as shown in Figure 5.2. The modules that are in operation are formed by an Arduino-based microprocessor that does all the process of data acquired by an ADXL355 MEMS accelerometer, from Analog Devices Company.

The sampling frequency rate considered for this application was set to 60 Hz. The data was collected in periods of 10 minutes and saved locally on a microSD card (Ietka, I. [et al.], 2023).

The modules, Figure 5.3, are powered by 9 lithium batteries of 3400 mAmps capacity and, as the wireless data transmission is disabled it permits a battery saving, allowing an overall nominal autonomy of 6 months. There is no synchronization between the two modules, because the location of the accelerometers is inside of the box girder beam, where is not possible to have GPS signal. Therefore, the synchronization was done in the post-processing stage.

Figure 5.3 - Accelerometer modules.

In Figure 5.4, it is possible to observe the variation in acceleration levels during two distinct periods: at night, characterized by lower excitation, and during the morning rush hour, marked by high traffic levels on the bridge.

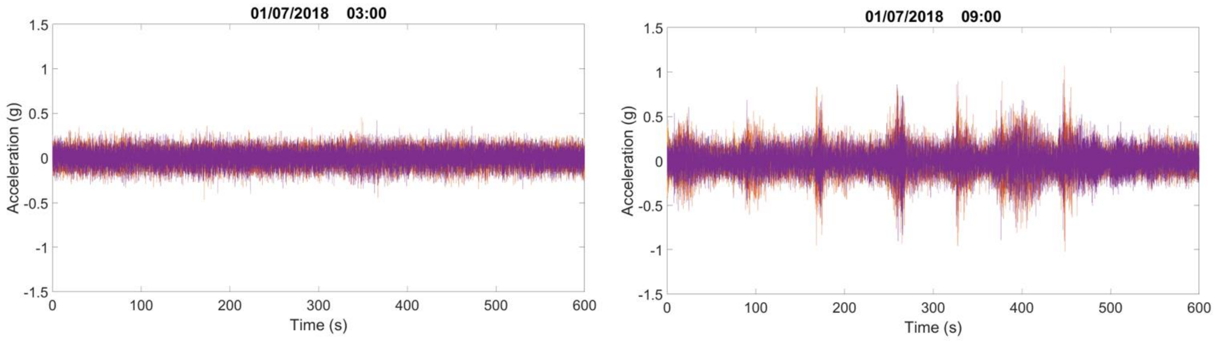

Figure 5.4 - Acceleration time series during the night (left) and the morning (right).

5.3. Automated Modal Parameter Selection

The stabilization diagram presented in Figure 5.5, obtained with PolyMax (subsection 2.1.2) represents the results of a measurement before the automated modal parameter selection (AMPS) methodology, covered in more detail in section 3.1. The measurement, with a sampling period of 10 minutes, is related to one of the rush hour periods in the Infante Dom Henrique bridge, in this case 5:10pm. It is possible to see a clear and clean stabilization diagram due to the higher excitation in this period.

To obtain the stabilization diagrams presented in Figure 5.5 and Figure 5.6, it was set a model size of 152, an exponential window of 1% was used to minimize leakage errors (Peeters, B. [et al.], 2007), and time lags of 7168.

In the Figure 5.6 is shown the same stabilization diagram as the one in Figure 5.5, but in this case after the AMPS methodology. It is possible to visualize the 13 natural frequencies identified in previous studies (Magalhães, F. [et al.], 2009). It is possible to see noise points identified by DBSCAN (subsection 3.1.1), as -1, that clearly does not represent a physical cluster. The physical clusters are coloured and present pink crosses, that represent the chosen representative poles.

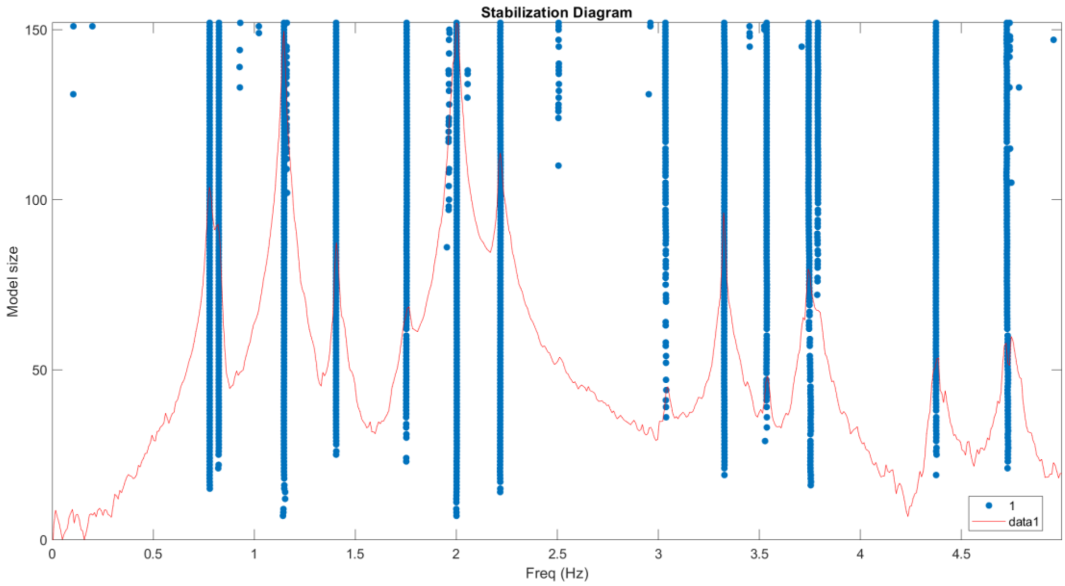

Figure 5.5 - Stabilization diagram of the bridge before AMPS methodology.

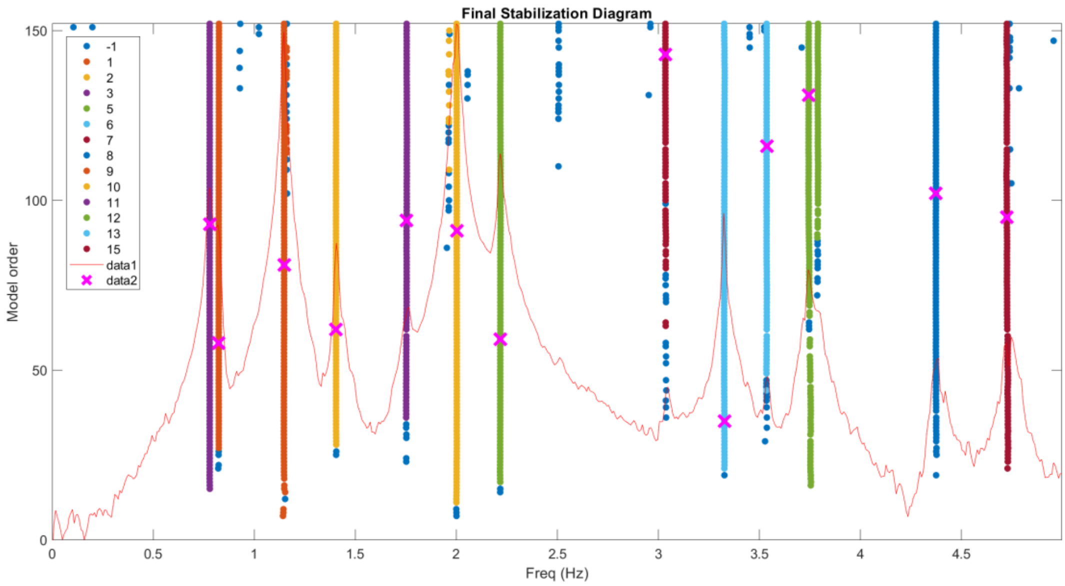

Figure 5.6 - Stabilization Diagram of the bridge after AMPS methodology.

Figure 5.7 displays a stabilization diagram of a measurement wherein not all natural frequencies are clearly identified. However, in proximity to the frequency of 3.03 Hz, a resonance frequency of the bridge is observed. This resonance frequency exhibits only one mode for that specific frequency. In the second verification step of the AMPS methodology (subsection 3.1.3), the column of poles representing the eliminated cluster, identified as -2, is recognized as a numerical one.

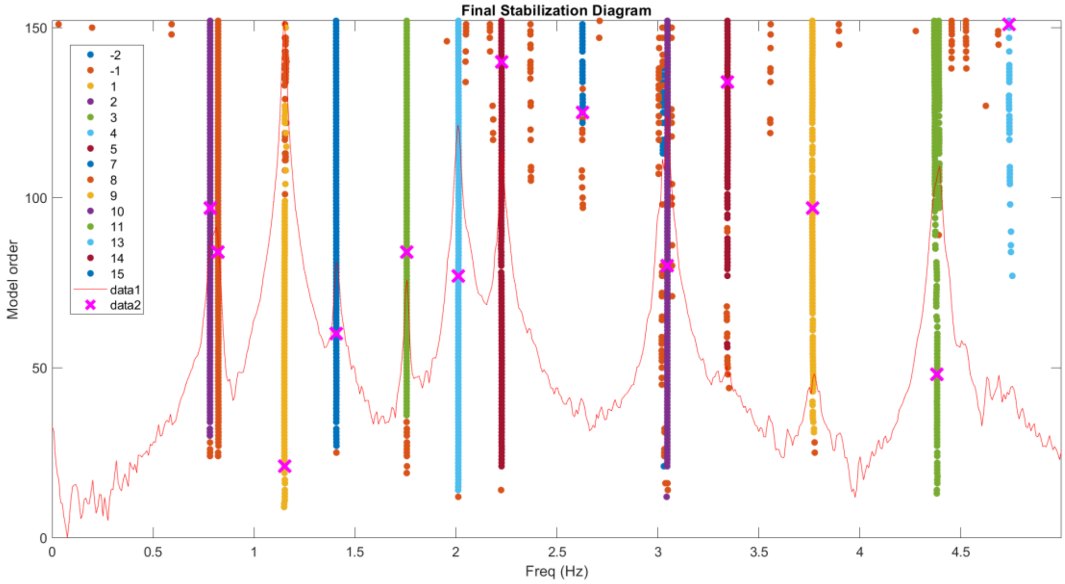

Figure 5.7 - Representative Stabilization Diagram of the Bridge for the Second Verification Step.

Table 5.1 and Table 5.2 present the vertical and bending modes, respectively, of the structure studied in this chapter. Due to the simplicity of the monitoring system described in subsection 5.2, it was not feasible to define completely the modes shapes, only the displacement of the points could be determined. In both tables, two different points are illustrated: the red points represent the lateral displacement at the sensor location, while the green points represent the vertical displacement. The images displayed behind the plotted points are derived from an Ambient Vibration Test conducted in a separate study, where the natural frequencies of the Infante Dom Henrique bridge were identified, and the mode shapes were calculated and displaced. Further information about the Ambient Vibration Test can be found in (Magalhães, F. [et al.], 2009).

In comparison to the referenced study, the adopted methodology in this research did not enable the correct identification of the modal configuration at the frequency of 2.0 Hz. Similarly, in the lateral bending, correspondence could not be established for the frequency of 3.31 Hz. This difficulty arises from the limitation of having only two sensors, which complicates the accurate identification of mode shapes.

Table 5.1 - Lateral view of four vertical bending modes.

f = 0.82 Hz 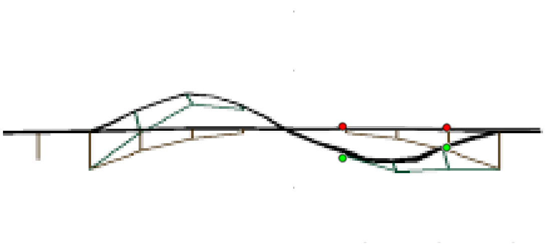	**f = 1.15 Hz** 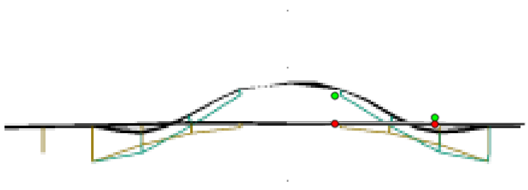
f = 1.40 Hz 	**f = 3.03 Hz** 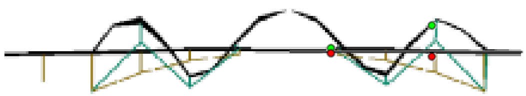

Table 5.2 - Top view of the two first lateral bending modes.

f = 0.78 Hz 	**f = 1.76 Hz** 

5.4. AUTOMATED MODAL TRACKING

The Automated Modal Tracking (AMT) is conducted following the approach described in the section 3.2. First, the global results of the AMPS methodology (subsection 3.1) for the entire month of July 2018 are depicted in Figure 5.8. Despite the noticeable presence of noise points, the graph clearly illustrates the thirteen prominent natural frequencies.

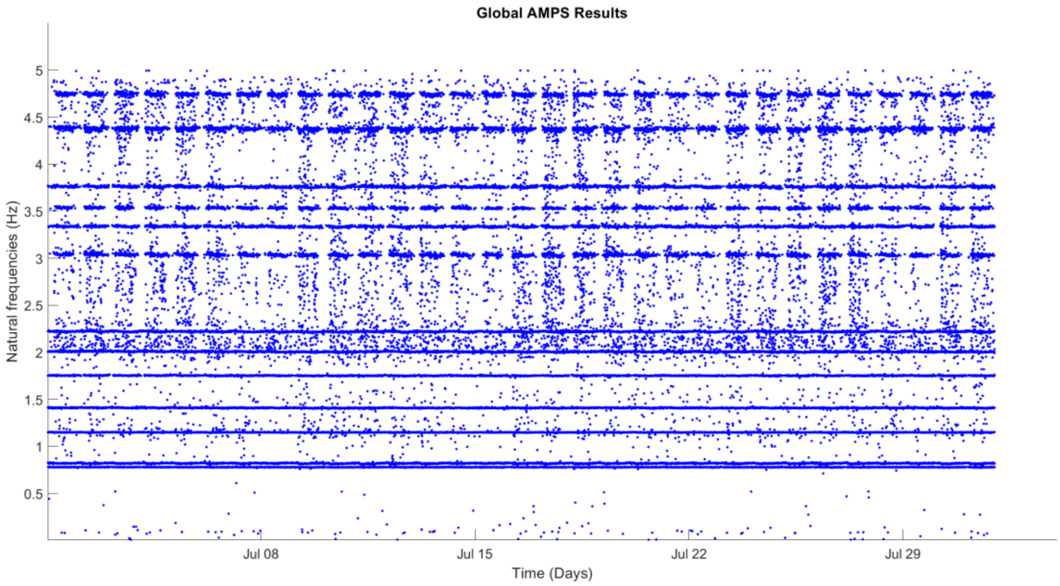

Figure 5.8 - AMPS Global Results of the bridge.

With the results of the AMPS methodology and a set of reference modes, it is possible to proceed to the last step of the Automated Modal Analysis (AMA) technique, the automated modal tracking. As a set of references, were considered the measurement showed in Figure 5.6, that is one of the measurements that best represent the thirteen modes of the Infante Dom Henrique bridge.

To perform the tracking of the structure under study in the present chapter, this one was performed only based in the distance frequency calculated as referred in section 3.2. Due to the simplicity of the monitoring system, which utilizes only two sensors, the MAC value will not be employed in this process because of the spatial aliasing phenomenon (He, M. [et al.], 2022). The MAC value will be just used in the case of existence of more than one possible match to the reference modes, in the same measurement. For the first six modes and the eighth one, a frequency distance variation of 0.02 was allowed. However, for the remaining modes, only a frequency distance variation of 0.015 was permitted due to the presence of more spurious modes around these frequencies, as shown in Figure 5.8.

An update of the reference modes was performed based on the 10 previous points in analysis, to adapt to small variations that could exist. This update of the reference is based on the average frequency of a certain number of previous points tracked, selecting the new reference as the one whose frequency value is closest to the average frequency among these points.

In Figure 5.9 and Figure 5.10 is shown the tracked natural frequencies and damping ratios per natural frequency, respectively, of the Infante Dom Henrique bridge, to the month of July 2018.

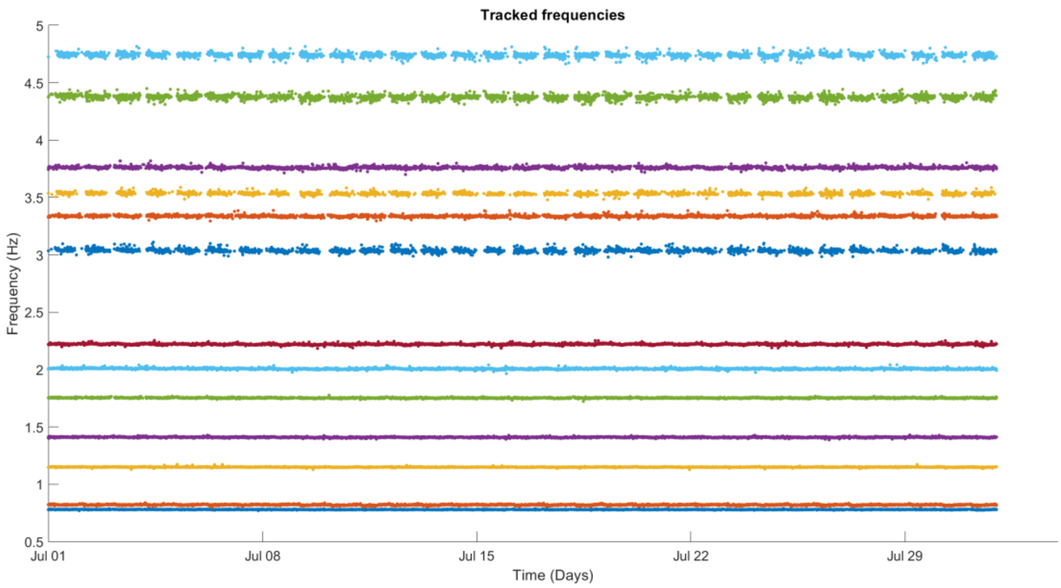

Figure 5.9 - Tracked frequencies for the Infante Dom Henrique Bridge in July 2018.

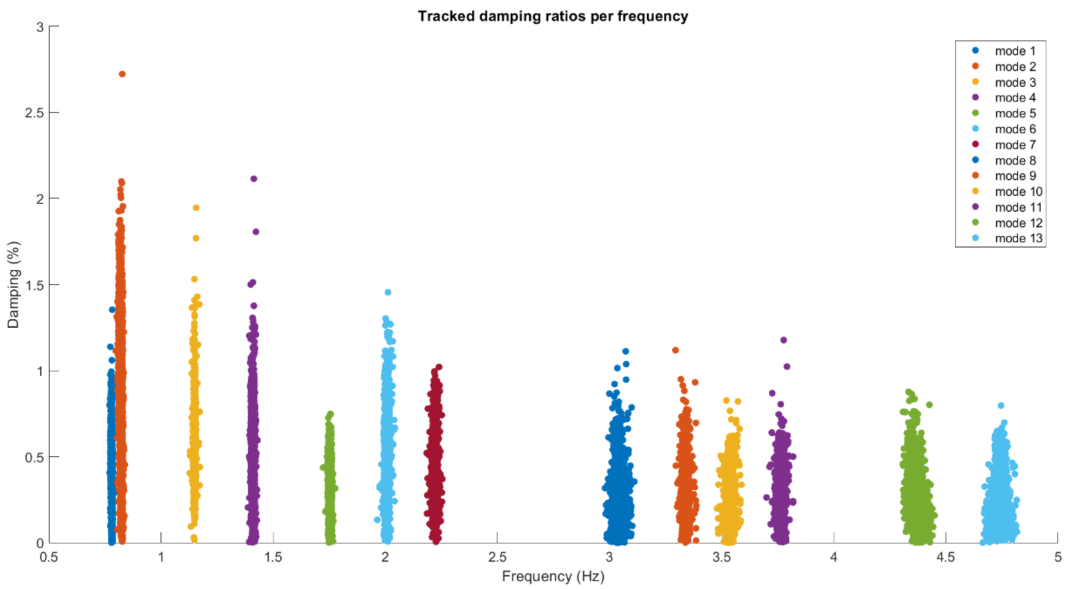

Figure 5.10 - Tracked damping ratios per frequency for the Infante Dom Henrique Bridge in July 2018.

The Table 5.3, show the outcomes of the modal tracking procedure, including the success rate, the mean natural frequency and damping ratio of every mode detected, and the correspondent standard deviation.

Table 5.3 - Results of the AMT methodology to the period of July 2018.

Modes	**Success Rate (%)**	$f_{mean}\ (Hz)$	$f_{std}\ (Hz)$	ξ_{mean} (%)	ξ_{std} (%)
1	89.00	0.7799	0.0016	0.3896	0.1457
2	94.94	0.8207	0.0041	0.8856	0.3286
3	99.98	1.1497	0.0022	0.4886	0.1560
4	95.72	1.4098	0.0035	0.4423	0.1992
5	89.42	1.7526	0.0033	0.3348	0.1084
6	99.62	2.0067	0.0051	0.4874	0.1729
7	98.63	2.2204	0.0054	0.4191	0.1321
8	54.72	3.0366	0.0143	0.2352	0.1519
9	82.30	3.3363	0.0074	0.3396	0.1240
10	53.98	3.5337	0.0099	0.2266	0.1186
11	84.27	3.7594	0.0084	0.3086	0.1116
12	70.78	4.3729	0.0171	0.2244	0.1306
13	64.49	4.7398	0.0156	0.2931	0.1231

Generally, the results presented are close to the ones presented in (de Magalhães, F.M.R.L., 2010). The success rates for the first 7 modes, 9^{th}, and 11^{th} achieve high values, and a clear definition of these modes is evident in Figure 5.9. However, for the remaining natural frequencies, some gaps are noticeable in Figure 5.9 , specifically in a metric-oriented manner. This reflects the lower success rate for these frequencies. These gaps primarily occur at higher frequencies due to reduced excitation during low rush hours, especially at night, which increases the difficulty in exciting the higher frequencies. This can be seen in the Figure 5.11, which represents a stabilization diagram of a low rush hour, specifically at 02:30 am. This occurs due to the higher noise levels of the accelerometers (subsection 5.2), which, given the lower excitation levels, do not allow for the capture of higher frequencies.

In the opposite scenario, the zones of good concentration of poles that are presented in this high frequencies (Figure 5.9) are tracked due to the high excitation during the rush hours because of the traffic (section 5.1). It is possible to see an example of a stabilization diagram representative of this situation in Figure 5.6.

Figure 5.10 shows the evolution of the tracked damping per frequency, where some damping values are close to zero due to the high levels of noise from the accelerometers used. This noise leads to the estimation of low values for measurements registered very close to the accelerometers' noise levels. Additionally, there is a wide range of damping values for each frequency, representing the natural vibration of the bridge due to the dynamic interaction between the bridge and the stopped vehicles on it (de Magalhães, F.M.R.L., 2010).

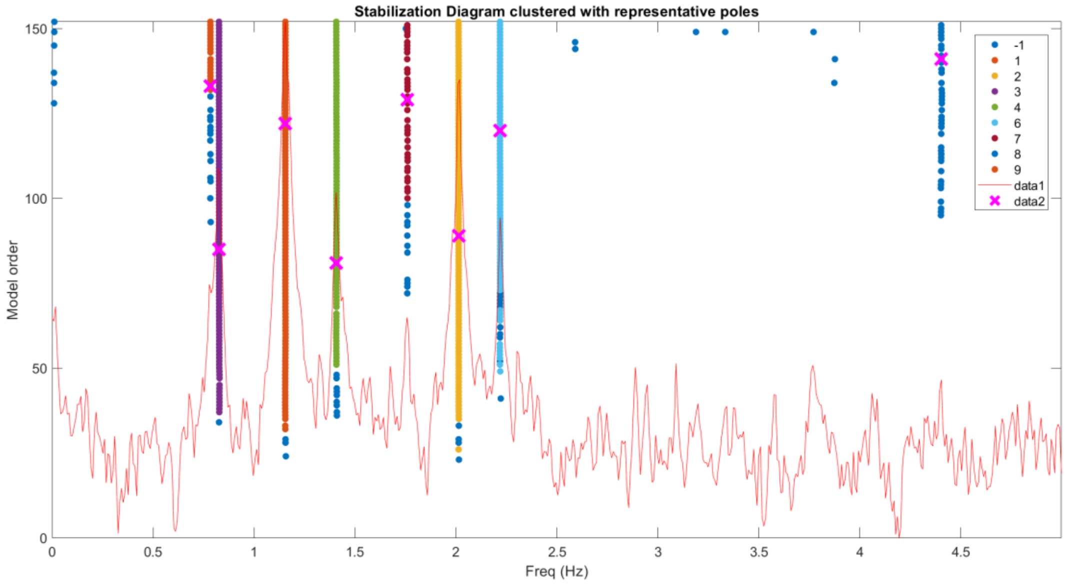

Figure 5.11 – Representative stabilization diagram of a low rush hour.

6
CONCLUSIONS

6.1. CONCLUSIONS

In this dissertation, an automated modal analysis (AMA) methodology utilizing Density-Based Spatial Clustering of Applications with Noise (DBSCAN) was successfully implemented within both Experimental Modal Analysis (EMA) and Operational Modal Analysis (OMA) contexts. The proposed methodology for Automated Modal Analysis (AMA) is divided into three crucial steps: Modal Parameter Estimation (MPE), Automated Modal Parameter Selection (AMPS) and Automated Modal Tracking (AMT). The AMPS method, based on DBSCAN, includes two additional verification steps. First, it merges clusters within the same frequency band that have similar characteristics. Second, it evaluates the contribution of each cluster to eliminate spurious modes. Afterwards, the AMT process is implemented to monitor the evolution of the modal parameters across the time.

Under EMA context, eight different industrial datasets were analysed using the Automated Modal Parameter Selection (AMPS) proposed in the AMA methodology. This approach demonstrated excellent results in extracting resonance modes from stabilization diagrams obtained with PolyMax for multiple structures such as a metallic plate, an airplane model, and an F16 jet. Additionally, the methodology was applied to five other datasets, including two motors, two fully trimmed cars, and a wind turbine blade, each subjected to different types of excitation and frequency ranges of analysis.

The results of this analysis were further validated through a benchmark study involving a group of engineers with varying levels of expertise in modal analysis. This benchmark validation was supported by a jury test composed of twenty-four engineers, divided into three expertise levels: novice, intermediate, and expert. These groups evaluated the eight industrial datasets, and their results were compared with those obtained through the AMPS methodology (DBSCAN) using various metrics, including the FRF synthesis error, the number of selected modes, the number of modes correlated with experts, and the number of modes uncorrelated with the experts.

The expert group, with over fifteen years of experience and significant contributions to the literature in the field, served as the benchmark for validating the results. Comparing the results obtained by the experts and the DBSCAN methodology, a high degree of similarity was observed in the FRF synthesis error, the number of selected modes, and the number of correlated modes. Only one mode was not correlated with those selected by the experts. This highlights the relevance of the AMPS methodology, particularly for novice and intermediate users, as it enhances the accuracy of modeset selection, which can otherwise be challenging due to their inexperience, providing better results. Even for expert users, this methodology offers the advantage of faster and equally reliable modeset selection compared to manual methods.

In the context of Operational Modal Analysis (OMA), long-term monitoring of the Infante Dom Henrique bridge was conducted using cost-effective accelerometers developed at FEUP. The sensor data were analyzed using the AMA methodology developed in this thesis.

During July 2018, the dynamic monitoring of the bridge reinforced the accuracy of the method used to estimate its modal parameters, achieving successful tracking throughout the month. However, the tracking exhibited gaps at higher frequencies due to a minor limitation of the accelerometers, that presents higher noise characteristics of the system, compared to the traditional ones. This limitation affected the ability to capture higher frequencies during low-traffic periods, especially at night when excitation levels were lower compared to morning and afternoon periods. Despite this, the methodology still produced good results, comparable to those obtained in a 2010 study on the same bridge. The tracking results were positive in terms of success rate, natural frequencies, and damping ratios.

Additionally, an example is provided to demonstrate how the second verification step of the AMPS methodology can reduce spurious modes in the Infante Dom Henrique bridge. This example highlights the utility of this step in improving results within an OMA context.

The mode shapes were also represented and compared with previous results obtained from an Ambient Vibration Test conducted in a 2010 study. Generally, it was possible to match the vertical and lateral bending of the structure at all frequencies with the mode shapes estimated from the data analyzed in this dissertation.

In summary, the AMA methodology developed in this thesis has demonstrated successful results in both EMA and OMA contexts.

6.2. FUTURE WORK

A very useful tool to perform Automated Modal Analysis (AMA) was studied in the present work, presenting successful results. However, full implementation and validation of the AMA methodology require consideration and analysis of several additional variables that can enhance the robustness of the method, such as:

- Preforming Automated Modal Analysis (AMA) using data from the accelerometers installed on the Infante Dom Henrique bridge for an entire year.
- Analysing other possible ways of calculating the contribution in the second verification step of the automated modal parameter selection (subsection 3.1.3).
- Applying the automated modal analysis methodology to other structures, especially in the operational modal analysis field.
- Investigating other sensors data, as the current study exclusively utilized acceleration data.

REFERENCES

Allemang, Randall J - The modal assurance criterion–twenty years of use and abuse. *Sound and vibration*. Vol. 37. n.º 8 (2003). p. 14-23. ISSN: 0022-460X

Avitabile, Peter - Modal testing: a practitioner's guide. John Wiley & Sons, 2017. ISBN: 1119222893

Boonyapinyo, Virote; Janesupasaeree, Tharach - Data-driven stochastic subspace identification of flutter derivatives of bridge decks. *Journal of Wind Engineering and Industrial Aerodynamics*. Vol. 98. n.º 12 (2010). p. 784-799. ISSN: 0167-6105

Brincker, Rune; Ventura, Carlos - Introduction to operational modal analysis. John Wiley & Sons, 2015. ISBN: 111996315X

Brincker, Rune; Zhang, Lingmi; Andersen, Palle - Modal identification from ambient responses using frequency domain decomposition. 2000. ISBN/ISSN:

Campello, Ricardo JGB; Moulavi, Davoud; Sander, Jörg - Density-based clustering based on hierarchical density estimates. Springer, 2013. ISBN/ISSN:

Center, Siemens Support - The Autopower Function… Demystified! 2020a. Disponível em WWW: <https://community.sw.siemens.com/s/article/the-autopower-function-demystified>. ISBN/ISSN:

Center, Siemens Support - OMG! What is OMA? Operational Modal Analysis. 2020b. Disponível em WWW: <https://community.sw.siemens.com/s/article/OMG-What-is-OMA-Operating-Modal-Analysis>. ISBN/ISSN:

Chen, WH; Lu, ZR; Lin, W; Chen, SH; Ni, YQ; Xia, Yong; Liao, WY - Theoretical and experimental modal analysis of the Guangzhou New TV Tower. *Engineering Structures*. Vol. 33. n.º 12 (2011). p. 3628-3646. ISSN: 0141-0296

de Magalhães, Filipe Manuel Rodrigues Leite - Operational modal analysis for testing and monitoring of bridges and special structures. Universidade do Porto (Portugal), 2010. ISBN/ISSN:

Dederichs, Anno C; Øiseth, Ole; Petersen, Øyvind W; Kvåle, Knut A - Comparison of automated operational modal analysis algorithms for long-span bridge applications. Springer, 2022. ISBN/ISSN:

Dederichs, Anno Christian; Øiseth, Ole - A novel and near-automatic mode tracking algorithm for civil infrastructure. *Journal of Sound and Vibration*. Vol. 573. (2024). p. 118217. ISSN: 0022-460X

Devriendt, Christof; Magalhães, Filipe; Weijtjens, Wout; De Sitter, Gert; Cunha, Álvaro; Guillaume, Patrick - Structural health monitoring of offshore wind turbines using automated operational modal analysis. *Structural Health Monitoring*. Vol. 13. n.º 6 (2014). p. 644-659. ISSN: 1475-9217

Di Lorenzo, Emilio - Operational Modal Analysis for rotating machines. Ph. D. Dissertation, Univ. of Naples Federico II, Naples, Italy, 2017. ISBN/ISSN:

Ester, Martin; Kriegel, Hans-Peter; Sander, Jörg; Xu, Xiaowei - A density-based algorithm for discovering clusters in large spatial databases with noise. 1996. ISBN/ISSN:

Favarelli, Elia; Giorgetti, Andrea - Machine learning for automatic processing of modal analysis in damage detection of bridges. *IEEE Transactions on Instrumentation and Measurement*. Vol. 70. (2020). p. 1-13. ISSN: 0018-9456

He, Min; Liang, Peng; Zhang, Yang; Yang, Fan; Liu, Jiu-xian - Unified method for fully automated modal identification and tracking with consideration of sensor deployment. *Engineering Structures*. Vol. 260. (2022). p. 114223. ISSN: 0141-0296

Heylen, Ward; Sas, Paul - Modal analysis theory and testing. (2006). ISSN:

Ietka, Isabelle; Moutinho, Carlos; Pereira, Sérgio; Cunha, Álvaro - Structural Monitoring of a Large-Span Arch Bridge Using Customized Sensors. *Sensors*. Vol. 23. n.º 13 (2023). p. 5971. ISSN: 1424-8220

Lau, Jenny; Lanslots, Jeroen; Peeters, Bart; Van der Auweraer, Herman - Automatic modal analysis. Reality or myth? *VDI BERICHTE*. Vol. 1982. (2007). p. 103. ISSN: 0083-5560

Magalhães, Filipe; Cunha, Álvaro - Explaining operational modal analysis with data from an arch bridge. *Mechanical systems and signal processing*. Vol. 25. n.º 5 (2011). p. 1431-1450. ISSN: 0888-3270

Magalhães, Filipe; Cunha, Alvaro; Caetano, Elsa - Online automatic identification of the modal parameters of a long span arch bridge. *Mechanical Systems and Signal Processing*. Vol. 23. n.º 2 (2009). p. 316-329. ISSN: 0888-3270

NV, Siemens Industry Software - Siemens Test.Lab Environmetal. 2015. ISBN/ISSN:

Oliveira, Gustavo; Magalhães, Filipe; Cunha, Álvaro; Caetano, Elsa - Continuous dynamic monitoring of an onshore wind turbine. *Engineering Structures*. Vol. 164. (2018). p. 22-39. ISSN: 0141-0296

Pastor, Miroslav; Binda, Michal; Harčarik, Tomáš - Modal assurance criterion. *Procedia Engineering*. Vol. 48. (2012). p. 543-548. ISSN: 1877-7058

Peeters, Bart; De Roeck, Guido - Reference-based stochastic subspace identification for output-only modal analysis. *Mechanical systems and signal processing*. Vol. 13. n.º 6 (1999). p. 855-878. ISSN: 0888-3270

Peeters, Bart; Van der Auweraer, Herman; Guillaume, Patrick; Leuridan, Jan - The PolyMAX frequency-domain method: a new standard for modal parameter estimation? *Shock and Vibration*. Vol. 11. n.º 3-4 (2004). p. 395-409. ISSN: 1070-9622

Peeters, Bart; Van der Auweraer, Herman; Vanhollebeke, Frederik; Guillaume, Patrick - Operational modal analysis for estimating the dynamic properties of a stadium structure during a football game. *Shock and Vibration*. Vol. 14. n.º 4 (2007). p. 283-303. ISSN: 1070-9622

Pereira, Sérgio; Reynders, Edwin; Magalhaes, Filipe; Cunha, Alvaro; Gomes, Jorge P - The role of modal parameters uncertainty estimation in automated modal identification, modal tracking and data normalization. *Engineering Structures*. Vol. 224. (2020). p. 111208. ISSN: 0141-0296

Rainieri, Carlo; Fabbrocino, Giovanni; Cosenza, Edoardo - An approach to automated modal parameter identification for structural health monitoring applications. 2008. ISBN/ISSN:

Reynders, Edwin; Houbrechts, Jeroen; De Roeck, Guido - Fully automated (operational) modal analysis. *Mechanical systems and signal processing*. Vol. 29. (2012). p. 228-250. ISSN: 0888-3270

Steenackers, Gunther; Guillaume, Patrick - Structural health monitoring of the Z24 Bridge in presence of environmental changes using modal analysis. 2005. ISBN/ISSN:

Tavares, André; Di Lorenzo, Emilio; Cornelis, Bram; Manzato, Simone; Peeters, Bart; Desmet, Wim; Gryllias, Konstantinos - Automated modal analysis through Machine Learning: an industrial validation. (2023). ISSN:

Tavares, André; Di Lorenzo, Emilio; Cornelis, Bram Manzato,Simone; Peeters, Bart ; Desmet, Wim; and Gryllias, Konstantinos - Automated modal analysis with density-based clustering: an industrial validation through jury testing. *Submited* (2024). ISSN:

Teng, Jun; Tang, De-Hui; Zhang, Xiao; Hu, Wei-Hua; Said, Samir; Rohrmann, Rolf G - Automated modal analysis for tracking structural change during construction and operation phases. *Sensors*. Vol. 19. n.º 4 (2019). p. 927. ISSN: 1424-8220

Verboven, Peter; Cauberghe, Bart; Parloo, Eli; Vanlanduit, Steve; Guillaume, Patrick - User-assisting tools for a fast frequency-domain modal parameter estimation method. *Mechanical systems and signal processing*. Vol. 18. n.º 4 (2004). p. 759-780. ISSN: 0888-3270

Verboven, Peter; Parloo, Eli; Guillaume, Patrick; Van Overmeire, Marc - Autonomous structural health monitoring—part I: modal parameter estimation and tracking. *Mechanical Systems and Signal Processing*. Vol. 16. n.º 4 (2002). p. 637-657. ISSN: 0888-3270

Zhang, Guowen; Ma, Jinghua; Chen, Zhuo; Wang, Ruirong - Automated eigensystem realisation algorithm for operational modal analysis. *Journal of Sound and Vibration*. Vol. 333. n.º 15 (2014). p. 3550-3563. ISSN: 0022-460X

Zhang, Guowen; Tang, Baoping; Tang, Guangwu - An improved stochastic subspace identification for operational modal analysis. *Measurement*. Vol. 45. n.º 5 (2012). p. 1246-1256. ISSN: 0263-2241